IRN Terascale @ IP21 Lyon

SModelS v3

Going Beyond Z_2 Topologies

Mohammad Mahdi Altakach

Based on: arXiv:2409.12942

S. Kraml, A. Lessa, S. Narasimha, T. Pascal, C. Ramos, Y. Villamizar and W. Waltenberger

14.11.2024

Outline

- Introduction
- SModelS: the concept
- SModelS: version 3
- Physics application
- Conclusions

Introduction

Introduction

- Searches for New Physics (**NP**) at the **LHC**:
  - **Channel-by-channel** in specific final states — **Only portion of the data**
  - Chosen set of **Simplified** ModelS (**SMS**) is tested — **Few of many new ideas**
- Phenomenologists' response:
  - **Combine** data from multiple analyses for more robust constraints
  - **Reinterpret** experimental results to explore a broader spectrum of theories

Introduction

- The **reuse** of experimental information is usually done in **2** ways:
  - **Recasting** of experimental analysis
    - Monte Carlo (**MC**) simulations are needed

CheckMATE 2, Rivet & Contur
MadAnalysis 5, ADL, ColliderBit, SimpleAnalysis

  - **Reuse of simplified model results**
    - Upper limit (**UL**) maps and Efficiency Maps (**EM**) are needed

SModelS : public tool for fast reinterpretation of **LHC** searches using simplified model results

This Talk

SModelS

the concept

SModelS working principle

- Decomposes the signatures of full **BSM** scenarios (particle content, masses, cross-sections, decay widths) into **simplified model components** with signal weights
- Confronts these components against the **experimental constraints** of the **SModelS** database
- Outputs presented as **r-values** (signal cross-section ratio to its upper limit)
- Also supports **global likelihood analyses** for more detailed statistical interpretations

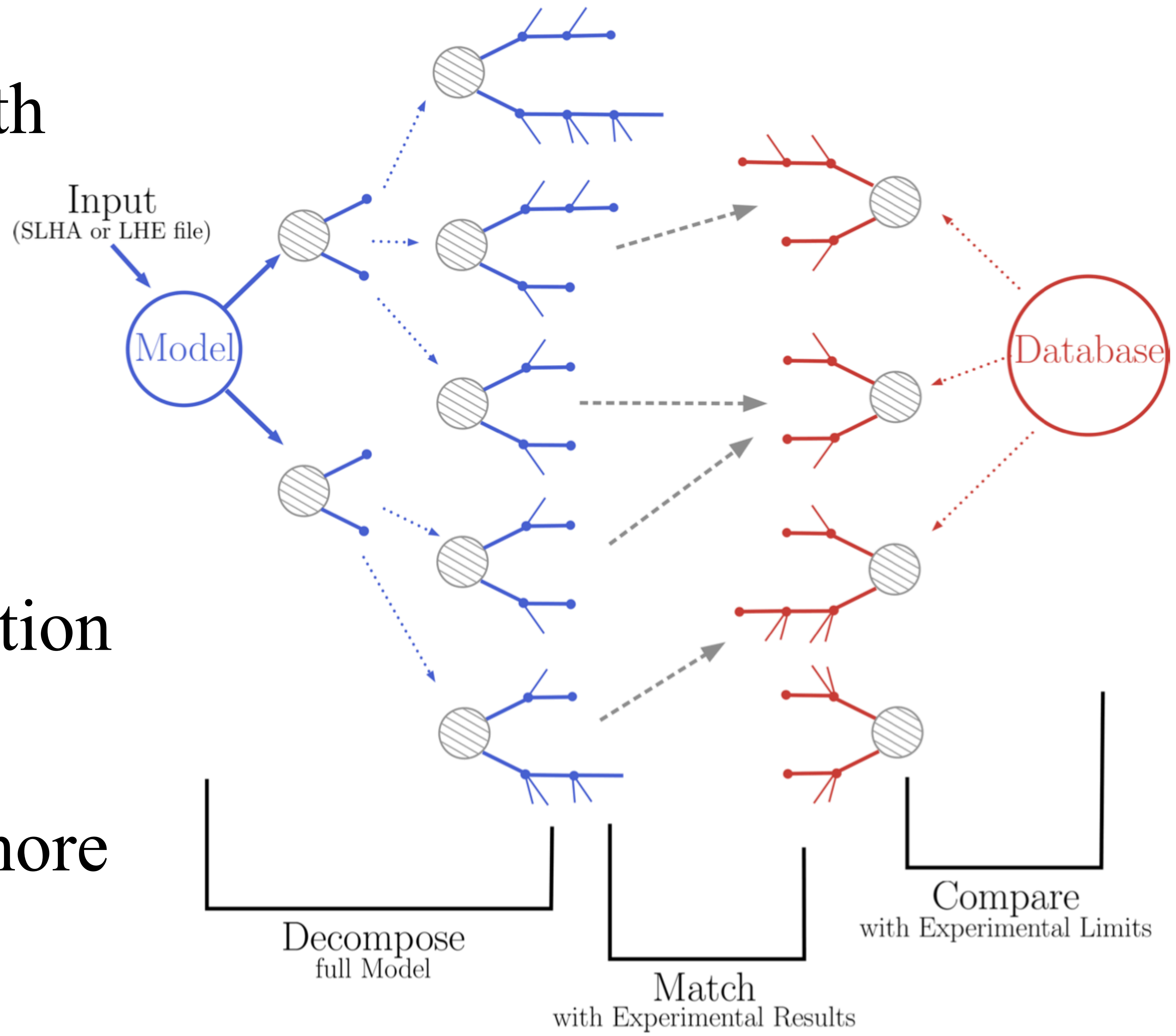

Pros & cons of SModelS

- **Advantages**:
  - High speed (no **MC** simulation needed) and ease of use
  - Suitable for model explorations and large parameter scans
  - Easy classification of unconstrained cross section (**missing topologies**)
- **Disadvantages**:
  - Kinematic distributions of the **signal** and **simplified model** should be similar enough
  - Limited to the **SMS** available in the database; larger database is needed for broader applicability
  - Recasting may offer **higher precision**, though at a **higher** computational **cost**

Experimental results used in SModelS

- **Upper limit** Type:
  - 95 % **CL upper limits on the signal cross section** (σ_{95}) as function of the simplified model parameters
  - $r = \left[\sigma \times BR \times BR\right] / \sigma_{95}$
  - Excluded if $r \geq 1$
  - Binary decision: excluded or not

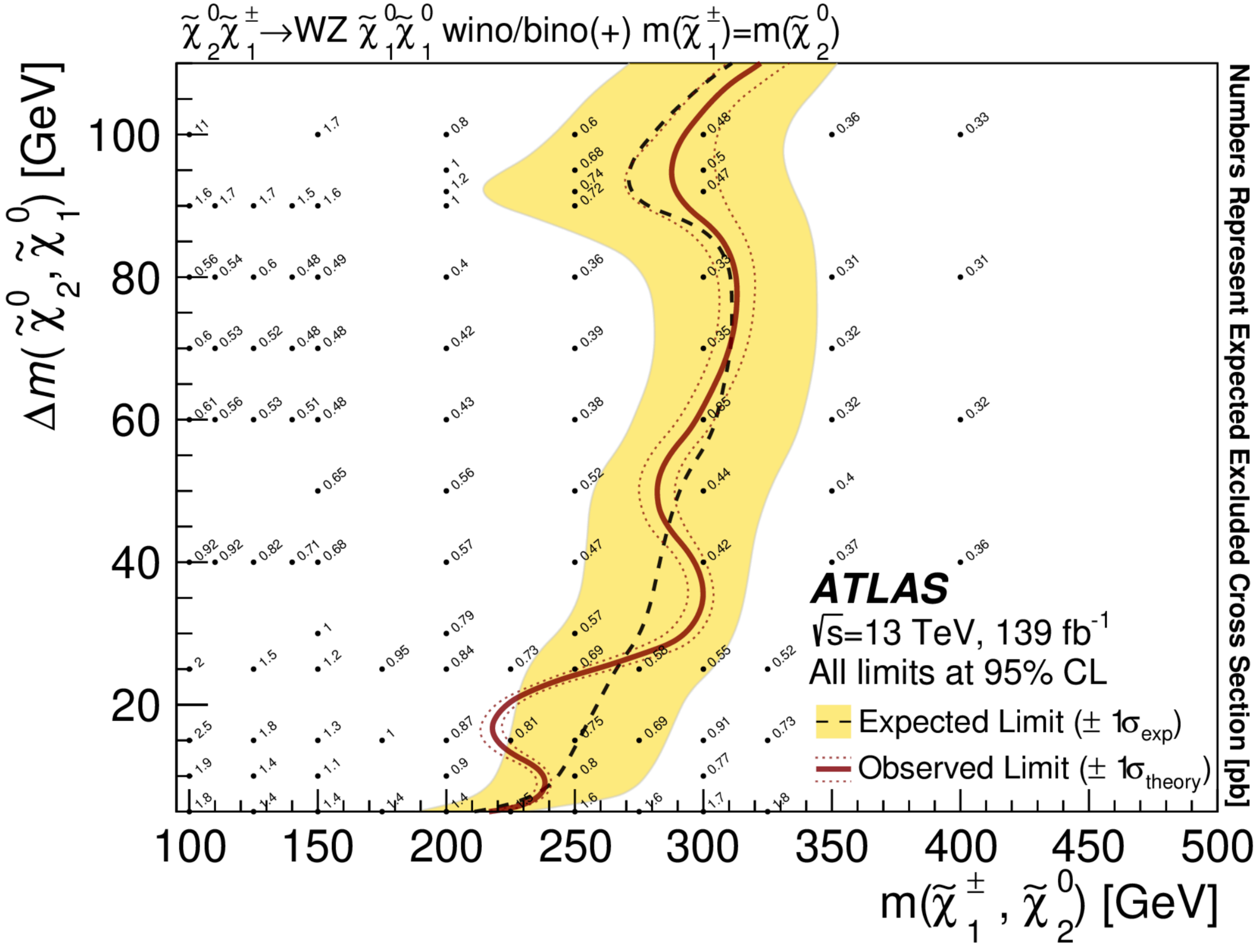

Experimental results used in SModelS

- **Efficiency maps** Type:
  - Acceptance (**A**) & Efficiency (ε) of each Signal Region (**SR**) as function of the simplified model parameters
  - **Different contributions** to the same **SR** can be added:
    $n_{sig} = A\epsilon \sum \left[\sigma \times BR \times BR\right] \times \mathscr{L}$
  - Given expected & observed number of events, the signal likelihood can be computed
  - Sophisticated statistical evaluations (likelihood ratio tests, CLs, …)

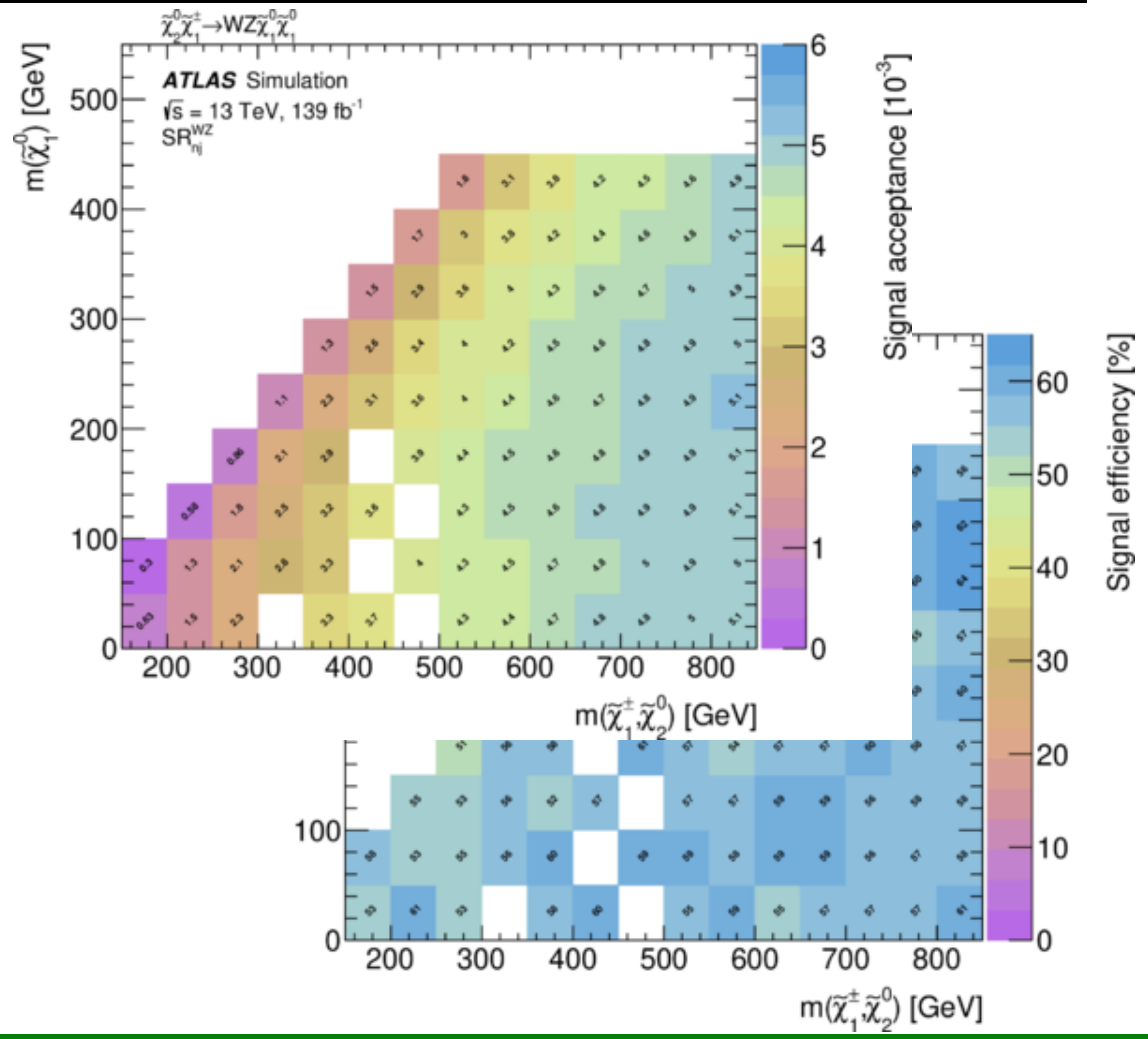

Combination of likelihoods

- Combination **of** **SR**:
  - Requires correlation info; without it, only the most sensitive **SR** can be used
  - **CMS**: covariance matrix, **ATLAS**: HistFactory model encoded in a json file
- Combination **of** **analyses**:
  - Assumes that those **analyses** are approximately uncorrelated
  - Combined likelihood is the product of the individual likelihoods from each analysis

Check T. Pascal's talk at Terascale @ LPSC Grenoble

SModelS: pre-version 3

- **Z_2** symmetry in **BSM** models:
  - Discrete symmetry distinguishing **SM** and **BSM** particles
  - Enforces **pair production** of BSM particles
- **Two-branch** Structure:
  - **Pair production** of **BSM** particles
  - Each **BSM** particle undergoes **cascade decays**, producing **SM** particles and terminating with the **LSP**

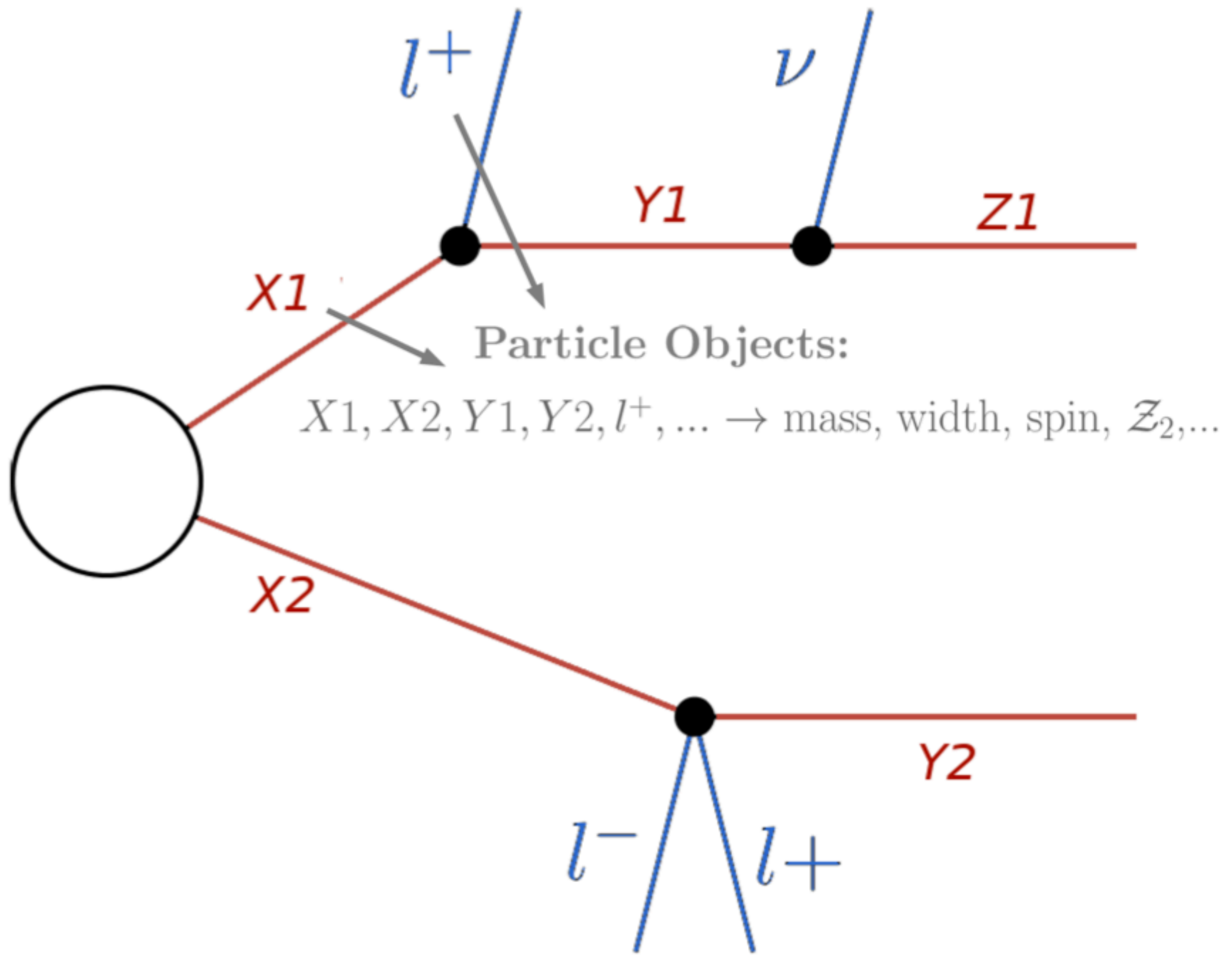

$[\,[X_1, Y_1, Z_1], [X_2, Y_2]\,]$

SModelS: pre-version 3

- **Limitations** of the **two-branch** structure:
  - Can't deal with **BSM** scenarios without new parity conservation (non-$\mathbf{Z_2}$ models):
    - Resonant (s-channel) production
    - Associated production **BSM** plus **SM** particles
    - Final states consisting of only **SM** particles

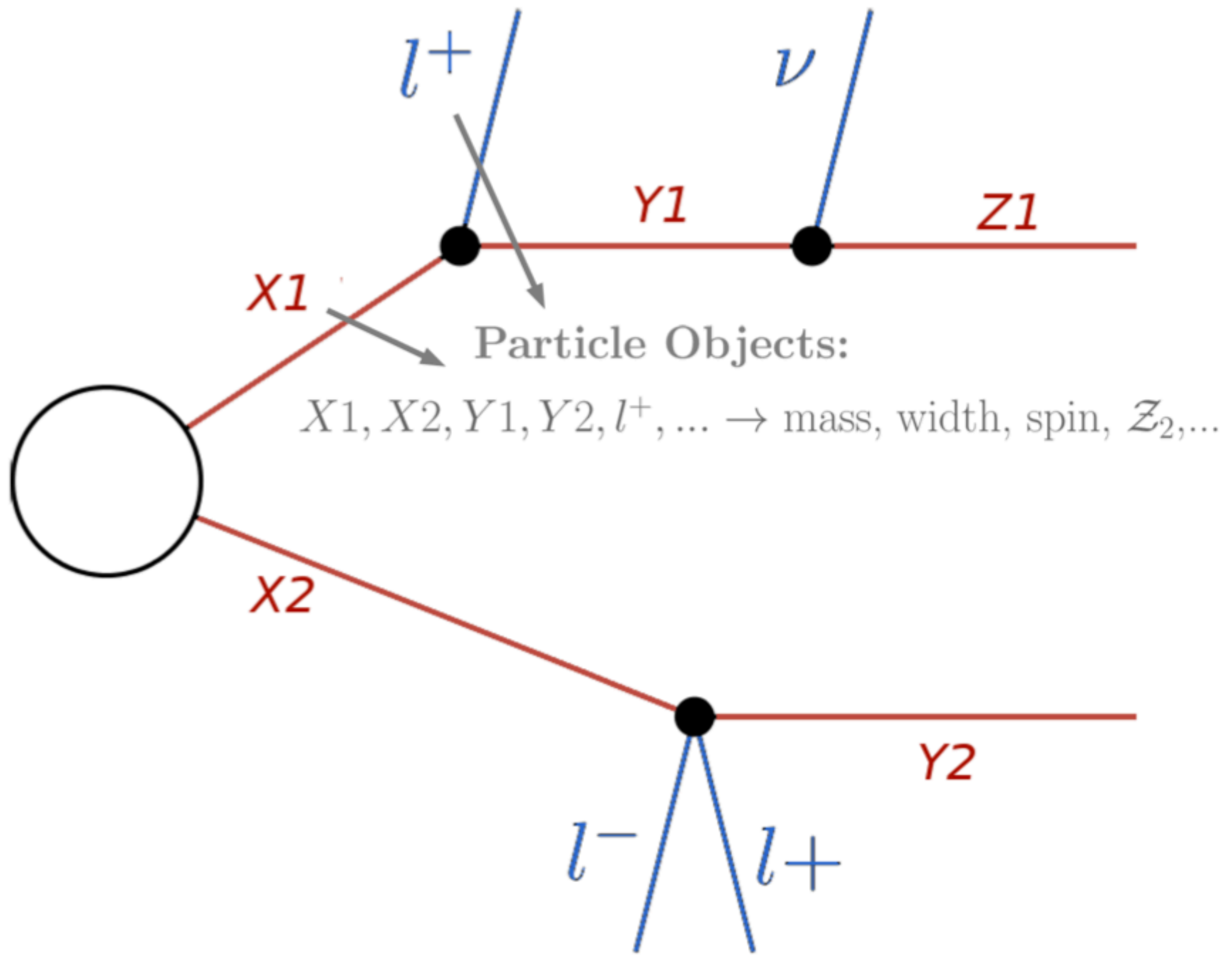

[[X_1, Y_1, Z_1], [X_2, Y_2]]

SModelS

version 3

SModelS: version 3

- **SModelS** is fully restructured; now relies on a **graph-based** description of simplified model topologies
- No need of an imposed $\mathbf{Z_2}$ symmetry
- Can handle **arbitrary** simplified model topologies

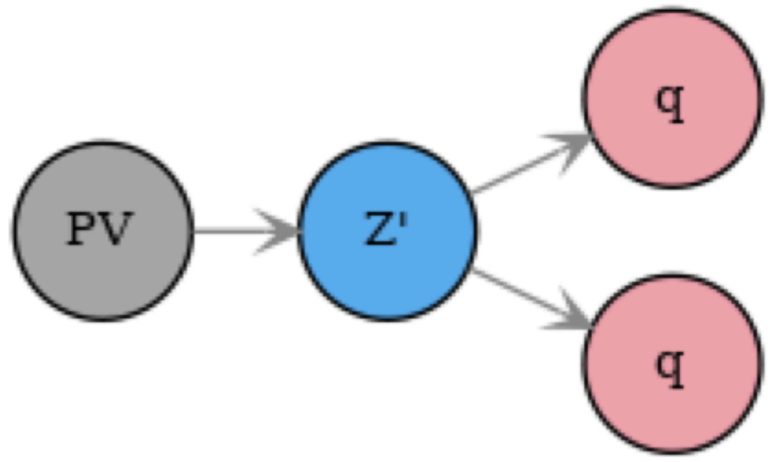

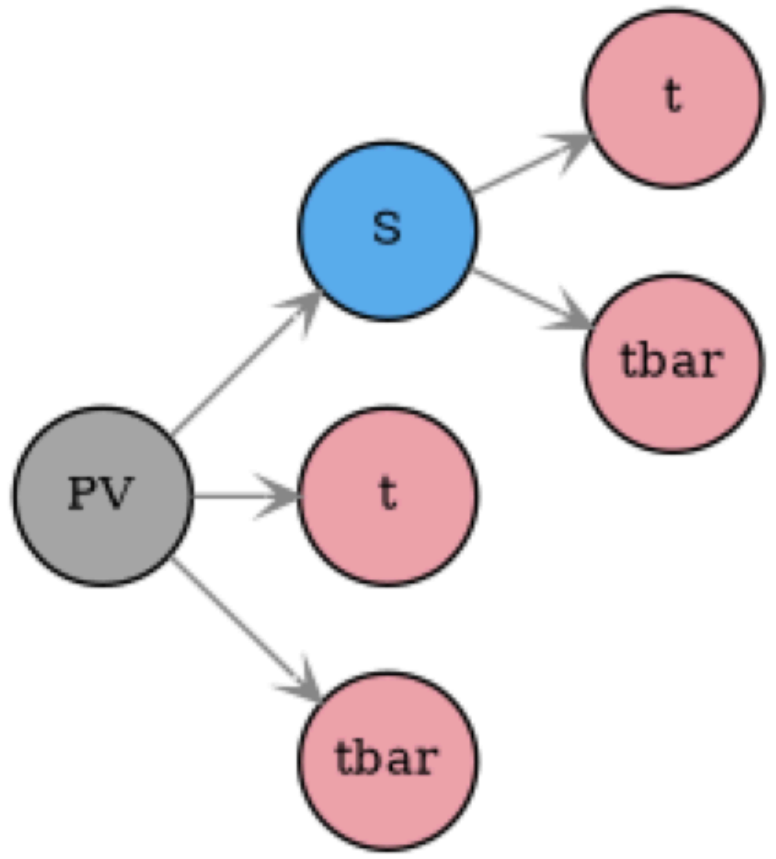

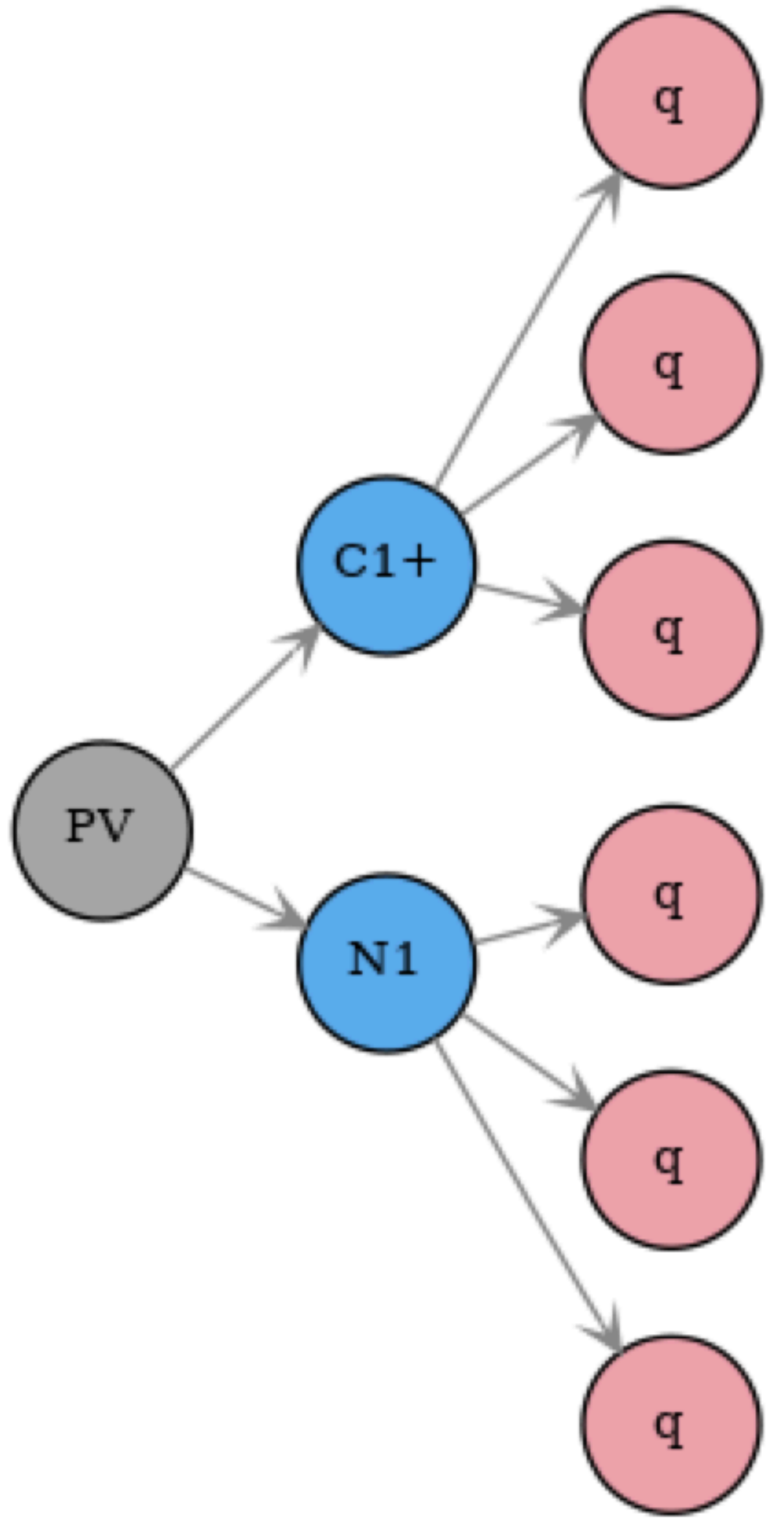

Graph-based topologies

- **Root node**: hard scattering (pp to produced particles)
- **Node**: particle appearing in the **SMS** topology
- **Node indices**: hold required information (Quantum Numbers (**QN**), mass, total width)
- Decays of **SM** particles not specified within the **graph** (given by **SM** values)
- A **graph** holds global info (the **SMS** weight)

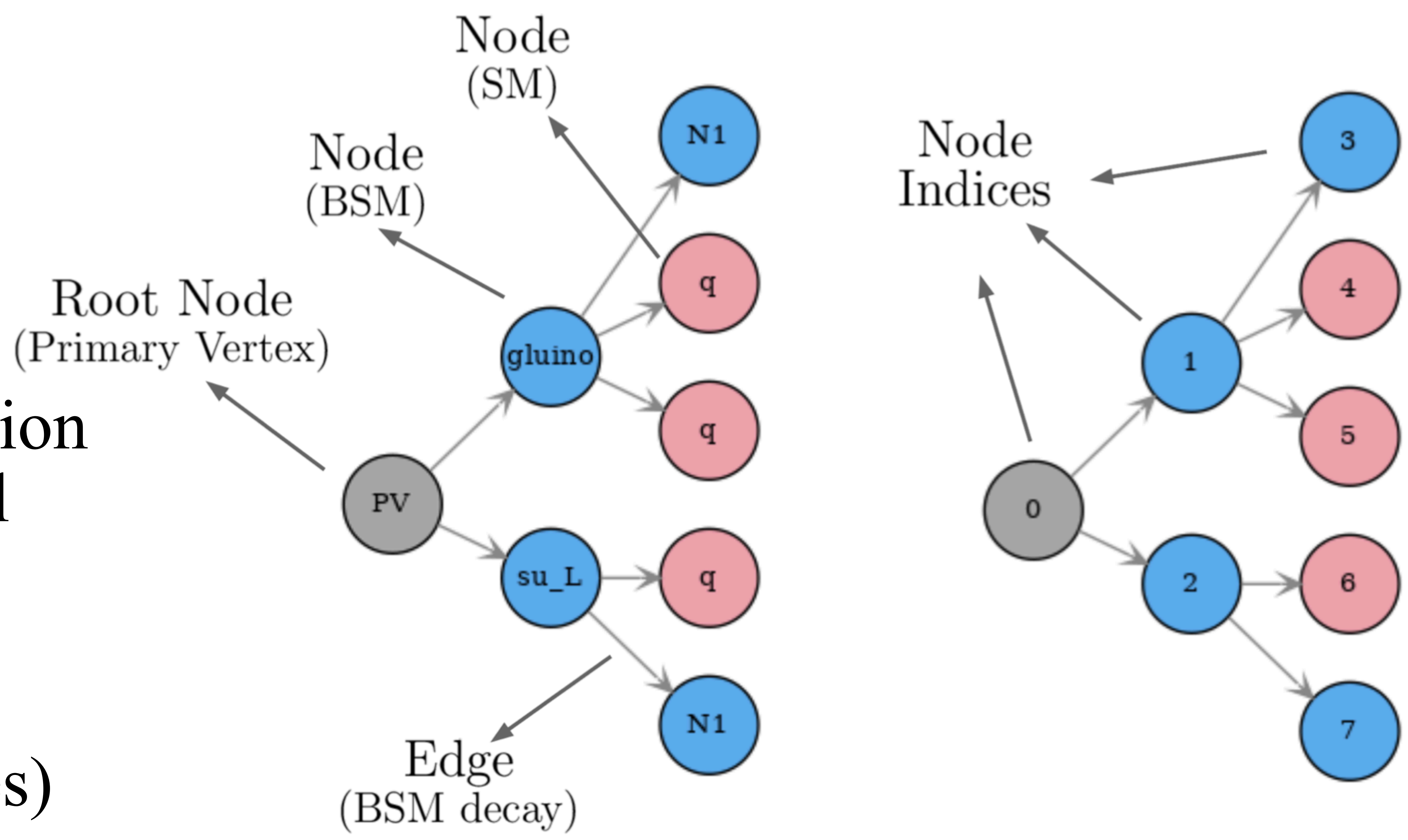

SMS matching

- **Matching** process:
  - Compare **SMS** topologies of the **input model** against those in the **SModelS database**.
- Criteria for matching topologies:
  - Same structure
  - Same particle properties
- Node matching:
  - Canonical names are equal
  - Particle attributes match
  - daughter nodes match, regardless of order

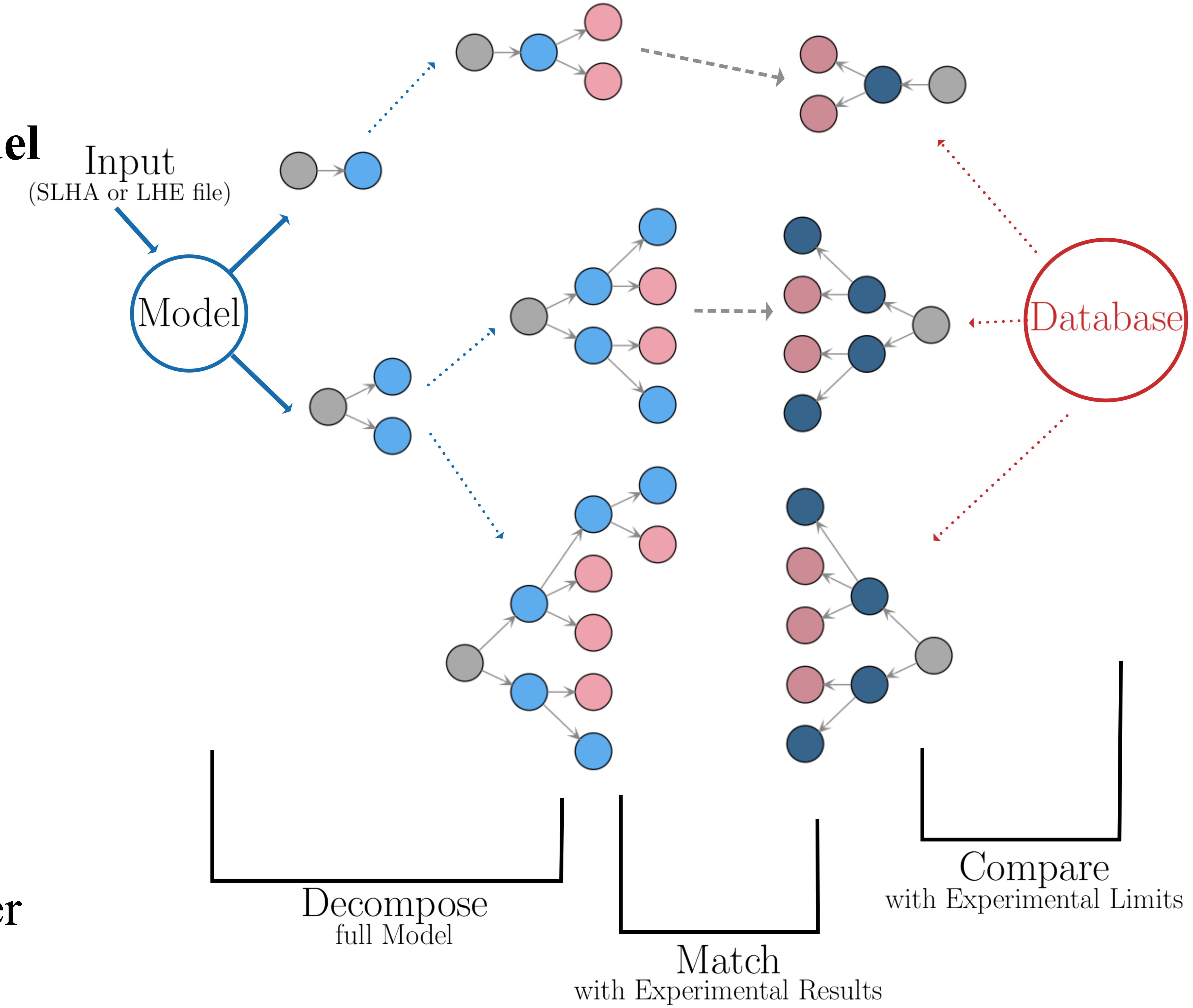

Physics application

Two-Mediator Dark Matter (2MDM) model

- Extends the SM gauge group with an additional $U(1)'$ symmetry
- New $U(1)'$ implies a new gauge boson (Z')
- A scalar field (ϕ) and a Majorana fermion (χ) are introduced
- Only the **SM** quarks are charged under $U(1)'$; their charges are universal

ψ	q_L	u_R	d_R	l_L	l_R	H	ϕ	χ	
U(1)$'$	q_q	q_q	q_q	0	0	0	q_ϕ	q_χ	← Charges

- The 3 **BSM** mass eigenstates are: Z', S and χ
- The independent model parameters are: $m_{Z'}$, m_S, m_χ, $g_\chi \equiv g_{Z'} q_\chi$, $g_q \equiv g_{Z'} q_q$ and $\sin\alpha$
  - $g_{Z'}$: gauge coupling of $U(1)'$, α: mixing angle between **SM** h and S

LHC signals

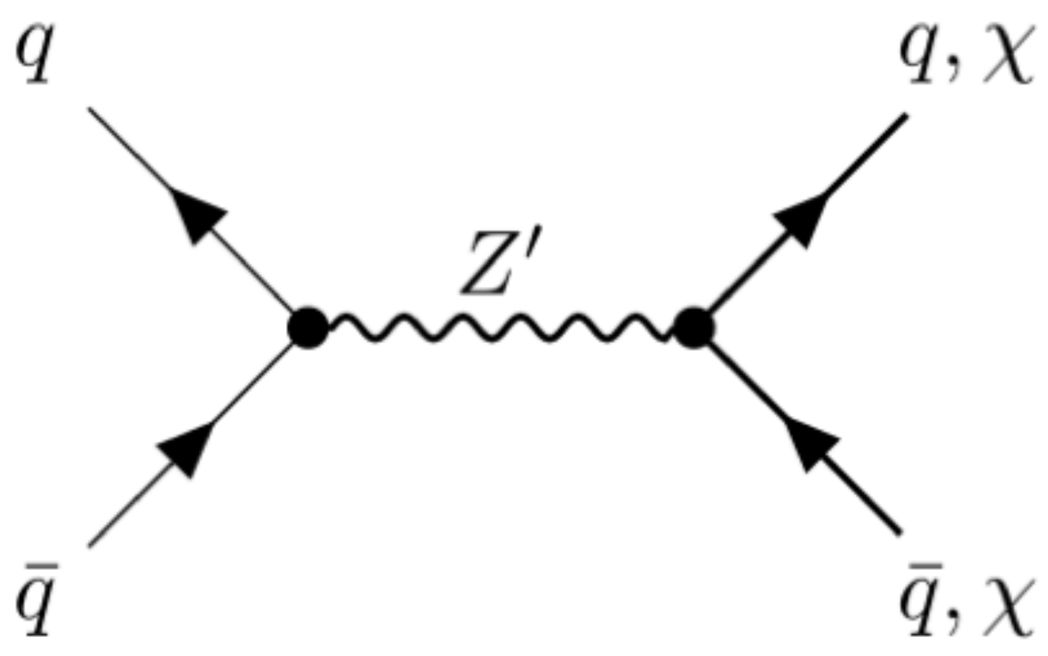

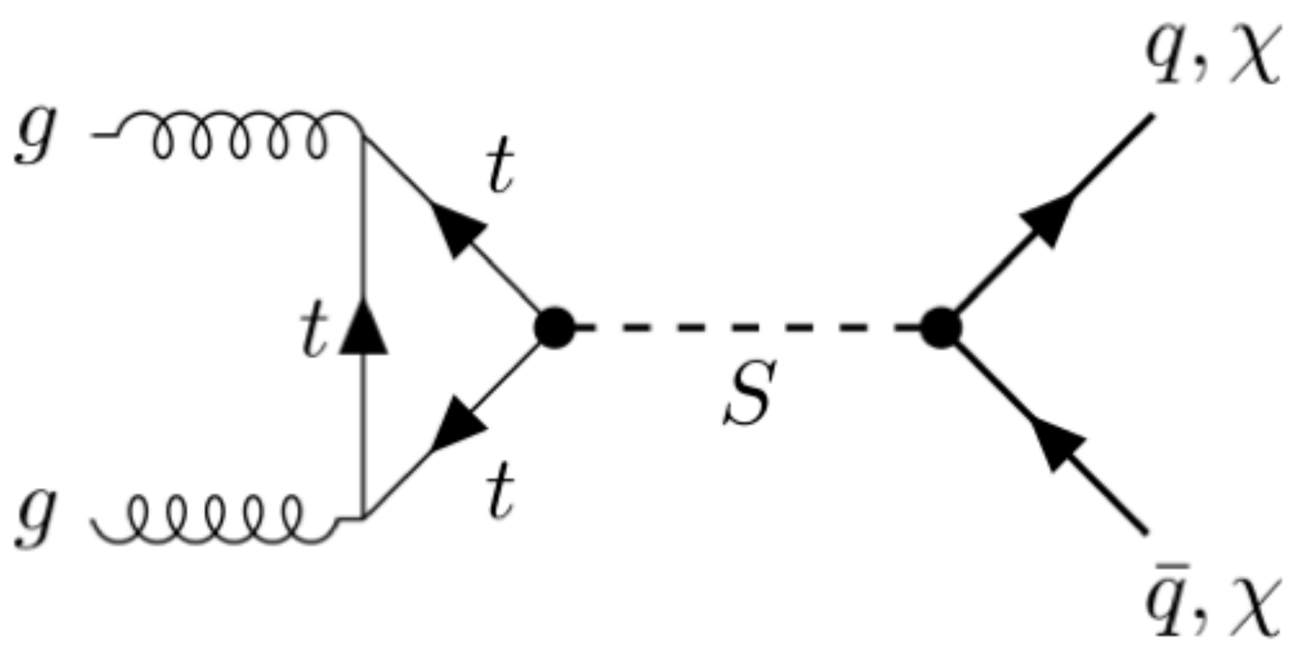

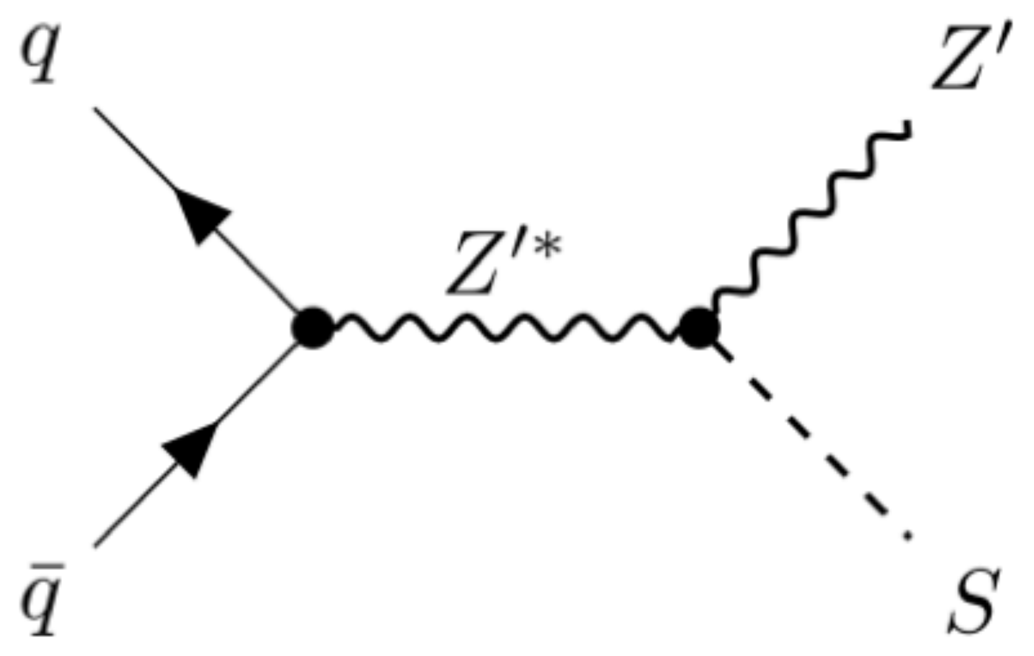

- The associated $Z'\,S$ production is always subdominant to the on-shell (s-channel) production of Z' ; **we don't take it into account**

LHC signals

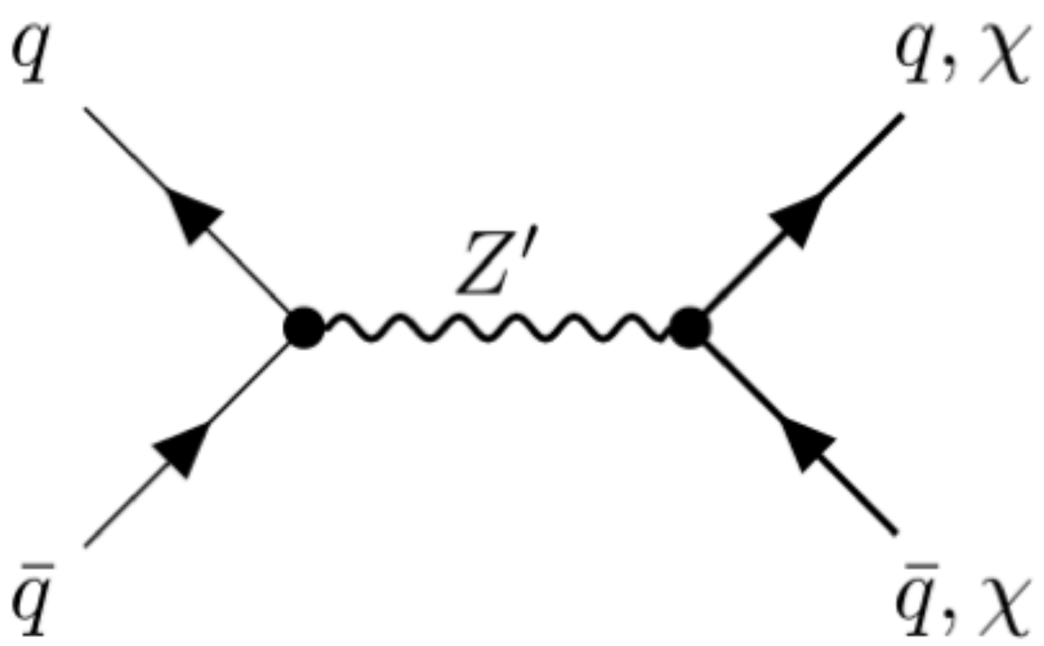

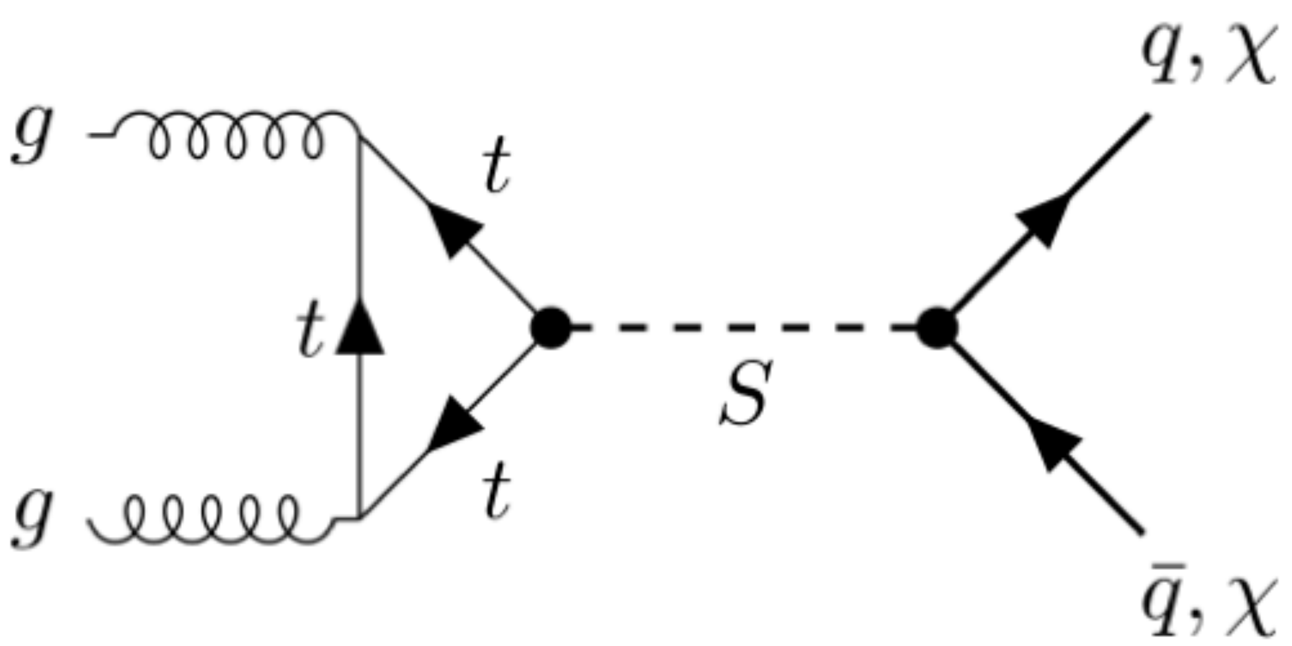

Process	Cross-Section
$pp \to Z' \to q\bar{q}$	$\sigma \propto g_q^4$
$pp \to Z' \to \chi\chi$	$\sigma \propto g_q^2 g_\chi^2$
$pp \to S \to q\bar{q}$	$\sigma \propto y_t^2 y_q^2 \sin^4 \alpha$
$pp \to S \to \chi\chi$	$\sigma \propto y_t^2 y_\chi^2 \sin^2 2\alpha$

$$y_\chi = 2\sqrt{2}\, g_{Z'} q_\chi \frac{m_\chi}{m_{Z'}}$$

- The associated $Z'\,S$ production is always subdominant to the on-shell (s-channel) production of Z' ; **we don't take it into account**
- The relative importance of the di-quark and E_T^{miss} depends on:
  - g_q / g_χ for the Z' mediator
  - y_q / y_χ for the S mediator
- The S production is suppressed for a small value of α and by a loop factor; **we don't take it into account**

New results in the database

- The signal can be probed by di-quark (dijet, *bb*, *tt*) resonance searches & searches for E_T^{miss} + jets:

ID	Signature	Luminosity	SMS Topology	Type
		Run 2–13 TeV		
ATLAS-EXOT-2019-03 [12]	Dijet resonance	$139\,\mathrm{fb}^{-1}$	$pp \to Z' \to jj, b\bar{b}$	UL
ATLAS-EXOT-2018-48 [13]	$t\bar{t}$ resonance	$139\,\mathrm{fb}^{-1}$	$pp \to Z' \to t\bar{t}$	UL
CMS-EXO-19-012 [14]	Dijet resonance	$137\,\mathrm{fb}^{-1}$	$pp \to Z' \to jj, b\bar{b}$	UL
CMS-EXO-20-008 [15]	b-jet resonance	$138\,\mathrm{fb}^{-1}$	$pp \to Z' \to b\bar{b}$	UL
CMS-EXO-20-004 [16]	Monojet	$137\,\mathrm{fb}^{-1}$	$pp \to Z', S \to \chi\chi$	EM
ATLAS-EXOT-2018-06 [17]	Monojet	$139\,\mathrm{fb}^{-1}$	$pp \to Z' \to \chi\chi$	UL
ATLAS-SUSY-2018-22 [18]	Multi-jet plus E_T^{miss}	$139\,\mathrm{fb}^{-1}$	$pp \to Z' \to \chi\chi$	EM
ATLAS-SUSY-2018-13 [19]	Displaced jets	$139\,\mathrm{fb}^{-1}$	$pp \to \tilde{\chi}\tilde{\chi} \to jjj, jjj; \ldots$	EM
		Run 1–8 TeV		
CMS-EXO-16-057 [20]	b-jet resonance	$19.7\,\mathrm{fb}^{-1}$	$pp \to Z' \to b\bar{b}$	UL
CMS-EXO-12-059 [21]	Dijet resonance	$19.7\,\mathrm{fb}^{-1}$	$pp \to Z' \to jj$	UL
ATLAS-EXOT-2013-11 [22]	Dijet resonance	$20.3\,\mathrm{fb}^{-1}$	$pp \to Z' \to jj$	UL

New results in the database

- The signal can be probed by di-quark (dijet, *bb*, *tt*) resonance searches & searches for E_T^{miss} + jets:

ID	Signature	Luminosity	SMS Topology	Type
		Run 2–13 TeV		
ATLAS-EXOT-2019-03 [12]	Dijet resonance	$139\,\text{fb}^{-1}$	$pp \to Z' \to jj, b\bar{b}$	UL
ATLAS-EXOT-2018-48 [13]	$t\bar{t}$ resonance	$139\,\text{fb}^{-1}$	$pp \to Z' \to t\bar{t}$	UL
CMS-EXO-19-012 [14]	Dijet resonance	$137\,\text{fb}^{-1}$	$pp \to Z' \to jj, b\bar{b}$	UL
CMS-EXO-20-008 [15]	b-jet resonance	$138\,\text{fb}^{-1}$	$pp \to Z' \to b\bar{b}$	UL
CMS-EXO-20-004 [16]	Monojet	$137\,\text{fb}^{-1}$	$pp \to Z', S \to \chi\chi$	EM
ATLAS-EXOT-2018-06 [17]	Monojet	$139\,\text{fb}^{-1}$	$pp \to Z' \to \chi\chi$	UL
ATLAS-SUSY-2018-22 [18]	Multi-jet plus E_T^{miss}	$139\,\text{fb}^{-1}$	$pp \to Z' \to \chi\chi$	EM
ATLAS-SUSY-2018-13 [19]	Displaced jets	$139\,\text{fb}^{-1}$	$pp \to \tilde{\chi}\tilde{\chi} \to jjj, jjj; \ldots$	EM
		Run 1–8 TeV		
CMS-EXO-16-057 [20]	b-jet resonance	$19.7\,\text{fb}^{-1}$	$pp \to Z' \to b\bar{b}$	UL
CMS-EXO-12-059 [21]	Dijet resonance	$19.7\,\text{fb}^{-1}$	$pp \to Z' \to jj$	UL
ATLAS-EXOT-2013-11 [22]	Dijet resonance	$20.3\,\text{fb}^{-1}$	$pp \to Z' \to jj$	UL

Has width dependent results

di-quark resonance searches

New results in the database

- The signal can be probed by di-quark (dijet, *bb*, *tt*) resonance searches & searches for E_T^{miss} + jets:

ID	Signature	Luminosity	SMS Topology	Type
		Run 2–13 TeV		
ATLAS-EXOT-2019-03 [12]	Dijet resonance	$139\,\mathrm{fb}^{-1}$	$pp \to Z' \to jj, b\bar{b}$	UL
ATLAS-EXOT-2018-48 [13]	$t\bar{t}$ resonance	$139\,\mathrm{fb}^{-1}$	$pp \to Z' \to t\bar{t}$	UL
CMS-EXO-19-012 [14]	Dijet resonance	$137\,\mathrm{fb}^{-1}$	$pp \to Z' \to jj, b\bar{b}$	UL
CMS-EXO-20-008 [15]	b-jet resonance	$138\,\mathrm{fb}^{-1}$	$pp \to Z' \to b\bar{b}$	UL
CMS-EXO-20-004 [16]	Monojet	$137\,\mathrm{fb}^{-1}$	$pp \to Z', S \to \chi\chi$	EM
ATLAS-EXOT-2018-06 [17]	Monojet	$139\,\mathrm{fb}^{-1}$	$pp \to Z' \to \chi\chi$	UL
ATLAS-SUSY-2018-22 [18]	Multi-jet plus E_T^{miss}	$139\,\mathrm{fb}^{-1}$	$pp \to Z' \to \chi\chi$	EM
ATLAS-SUSY-2018-13 [19]	Displaced jets	$139\,\mathrm{fb}^{-1}$	$pp \to \tilde{\chi}\tilde{\chi} \to jjj, jjj; \ldots$	EM
		Run 1–8 TeV		
CMS-EXO-16-057 [20]	b-jet resonance	$19.7\,\mathrm{fb}^{-1}$	$pp \to Z' \to b\bar{b}$	UL
CMS-EXO-12-059 [21]	Dijet resonance	$19.7\,\mathrm{fb}^{-1}$	$pp \to Z' \to jj$	UL
ATLAS-EXOT-2013-11 [22]	Dijet resonance	$20.3\,\mathrm{fb}^{-1}$	$pp \to Z' \to jj$	UL

E_T^{miss} + jets searches

Recasted

New results in the database

- The signal can be probed by di-quark (dijet, *bb*, *tt*) resonance searches & searches for E_T^{miss} + jets:

ID	Signature	Luminosity	SMS Topology	Type
		Run 2–13 TeV		
ATLAS-EXOT-2019-03 [12]	Dijet resonance	$139\,\text{fb}^{-1}$	$pp \to Z' \to jj, b\bar{b}$	UL
ATLAS-EXOT-2018-48 [13]	$t\bar{t}$ resonance	$139\,\text{fb}^{-1}$	$pp \to Z' \to t\bar{t}$	UL
CMS-EXO-19-012 [14]	Dijet resonance	$137\,\text{fb}^{-1}$	$pp \to Z' \to jj, b\bar{b}$	UL
CMS-EXO-20-008 [15]	b-jet resonance	$138\,\text{fb}^{-1}$	$pp \to Z' \to b\bar{b}$	UL
CMS-EXO-20-004 [16]	Monojet	$137\,\text{fb}^{-1}$	$pp \to Z', S \to \chi\chi$	EM
ATLAS-EXOT-2018-06 [17]	Monojet	$139\,\text{fb}^{-1}$	$pp \to Z' \to \chi\chi$	UL
ATLAS-SUSY-2018-22 [18]	Multi-jet plus E_T^{miss}	$139\,\text{fb}^{-1}$	$pp \to Z' \to \chi\chi$	EM
ATLAS-SUSY-2018-13 [19]	Displaced jets	$139\,\text{fb}^{-1}$	$pp \to \tilde{\chi}\tilde{\chi} \to jjj, jjj; \ldots$	EM
		Run 1–8 TeV		
CMS-EXO-16-057 [20]	b-jet resonance	$19.7\,\text{fb}^{-1}$	$pp \to Z' \to b\bar{b}$	UL
CMS-EXO-12-059 [21]	Dijet resonance	$19.7\,\text{fb}^{-1}$	$pp \to Z' \to jj$	UL
ATLAS-EXOT-2013-11 [22]	Dijet resonance	$20.3\,\text{fb}^{-1}$	$pp \to Z' \to jj$	UL

RPV SUSY search

Parameter scan

- **SLHA** format as input for **SModelS**:
  - **LO** cross-section for Z' production with **Madgraph**
  - $$\Gamma_{(Z' \to q\bar{q})} = \frac{g_q^2 m_{Z'}}{4\pi} \sqrt{1 - \frac{4m_q^2}{m_{Z'}^2}} \left(1 + \frac{2m_q^2}{m_{Z'}^2}\right)$$
  - $$\Gamma_{(Z' \to \chi\chi)} = \frac{g_\chi^2 m_{Z'}}{24\pi} \left(1 - \frac{4m_\chi^2}{m_{Z'}^2}\right)^{\frac{3}{2}}$$

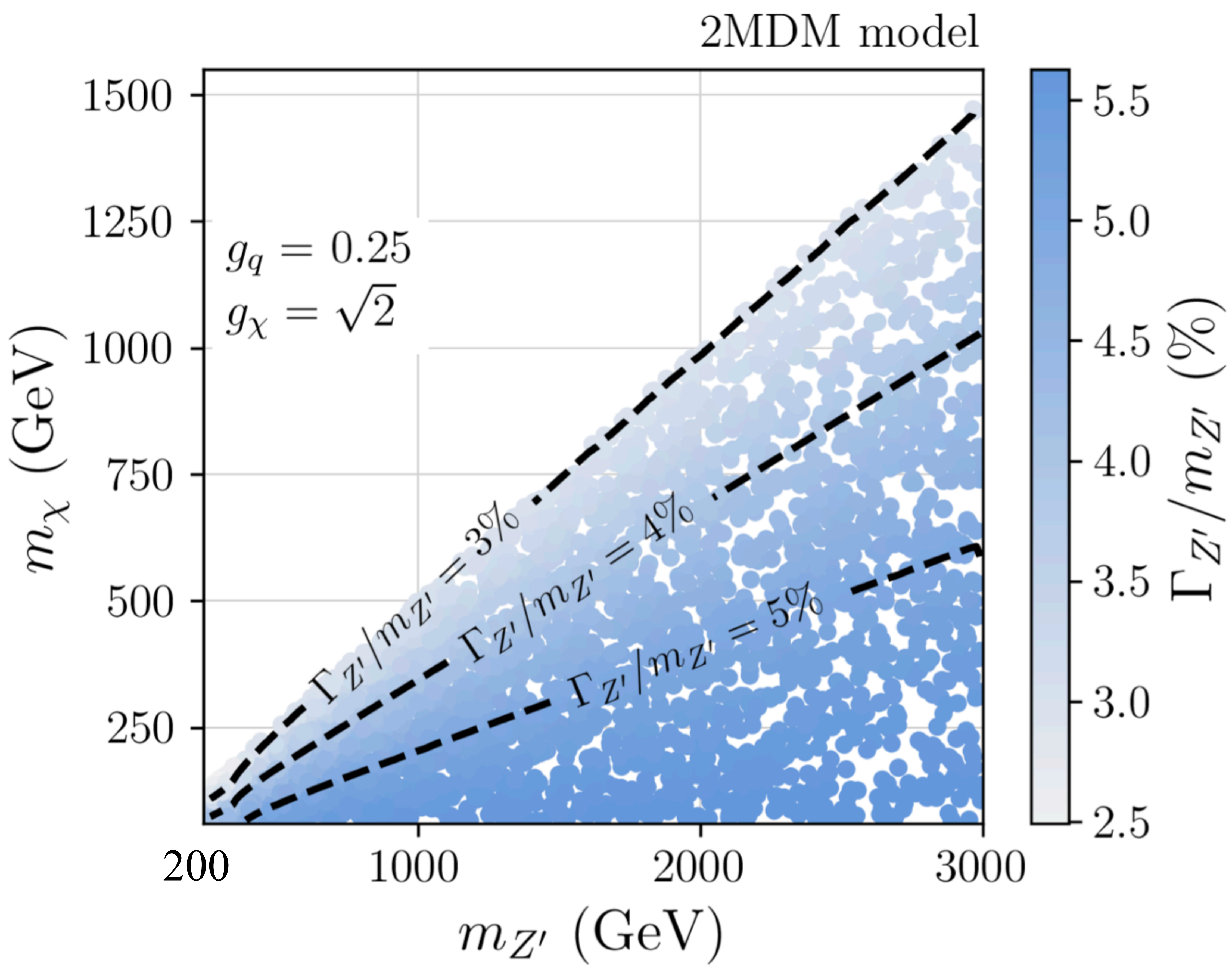

Constraints from jets + MET searches

- Observed & expected exclusions:
  - Observed weaker than expected for ATLAS multijet & CMS; data > **SM** background
  - CMS: highest sensitivity (strongest expected limit) & weaker observed limit; largest over-fluctuations
  - BR($Z' \to \chi\chi$) decreases with increasing m_χ; loss of sensitivity close to $m_{Z'} = 2m_\chi$

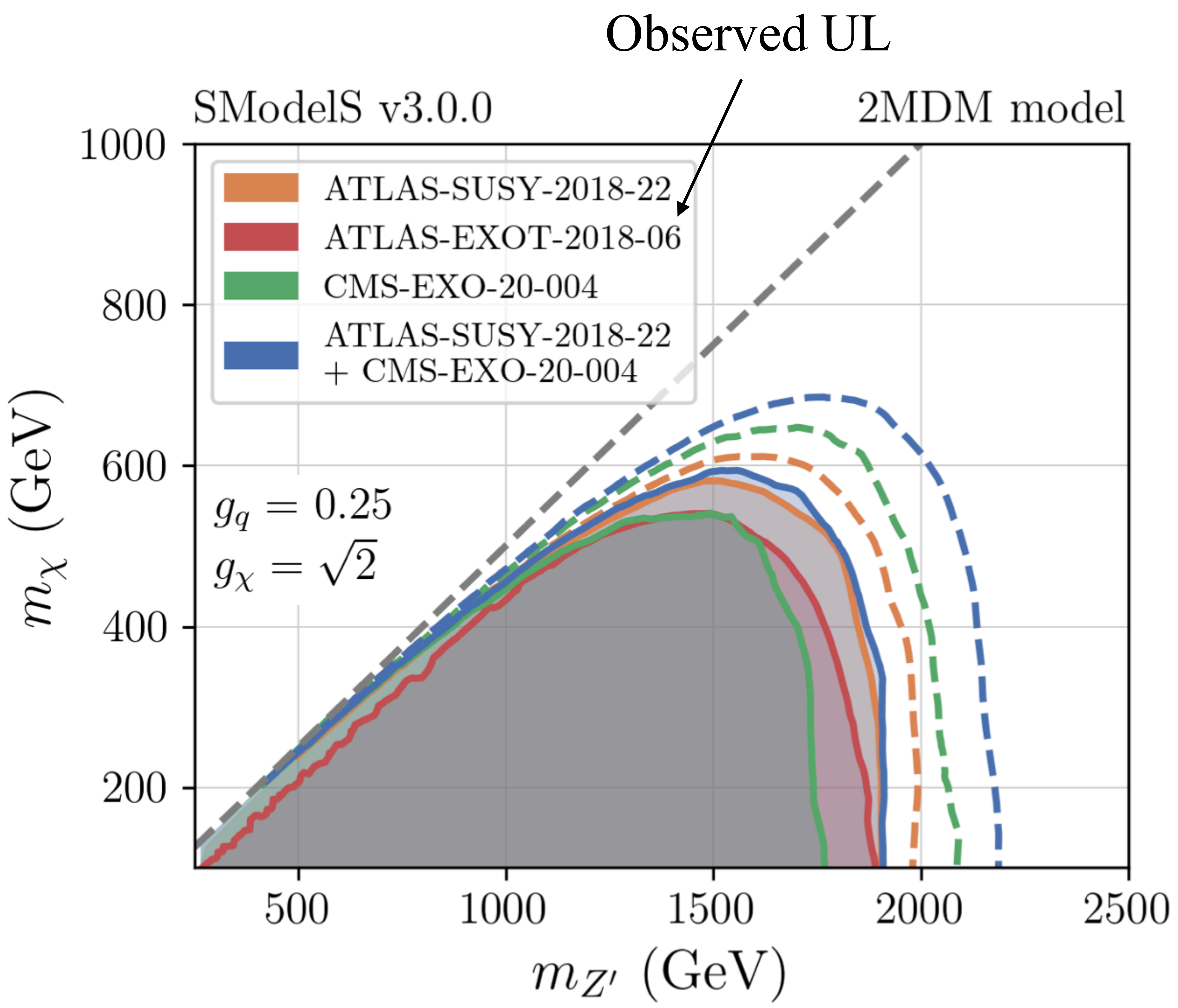

Constraints from jets + MET searches

- Observed & expected exclusions (combined):
  - The combination extends the expected reach by 100 – 200 GeV
  - The combination observed exclusion is almost the same as the ATLAS multijet case
    - A more robust limit is obtained

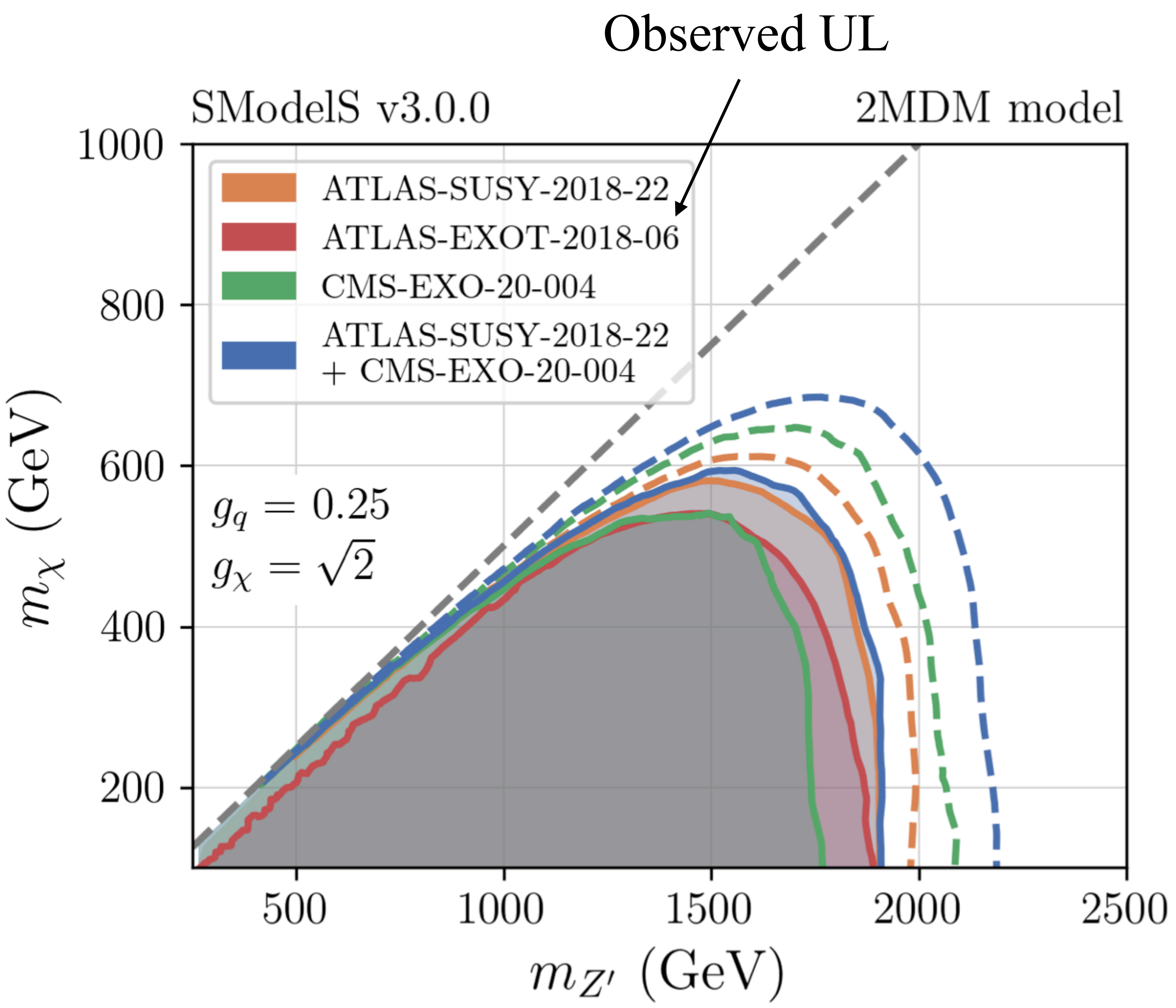

Constraints from jets + MET searches

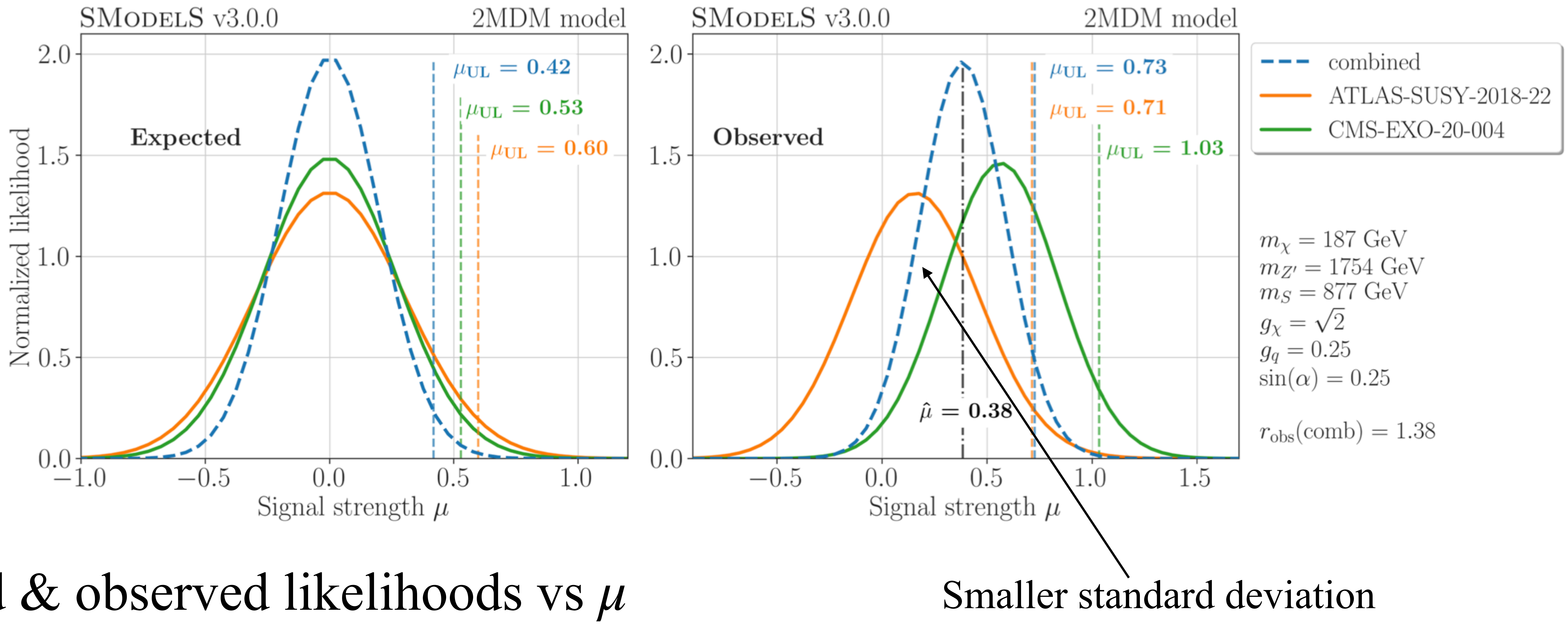

- Expected & observed likelihoods vs μ
  - $r = 1/\mu_{UL}$

Resonance vs jets + MET searches

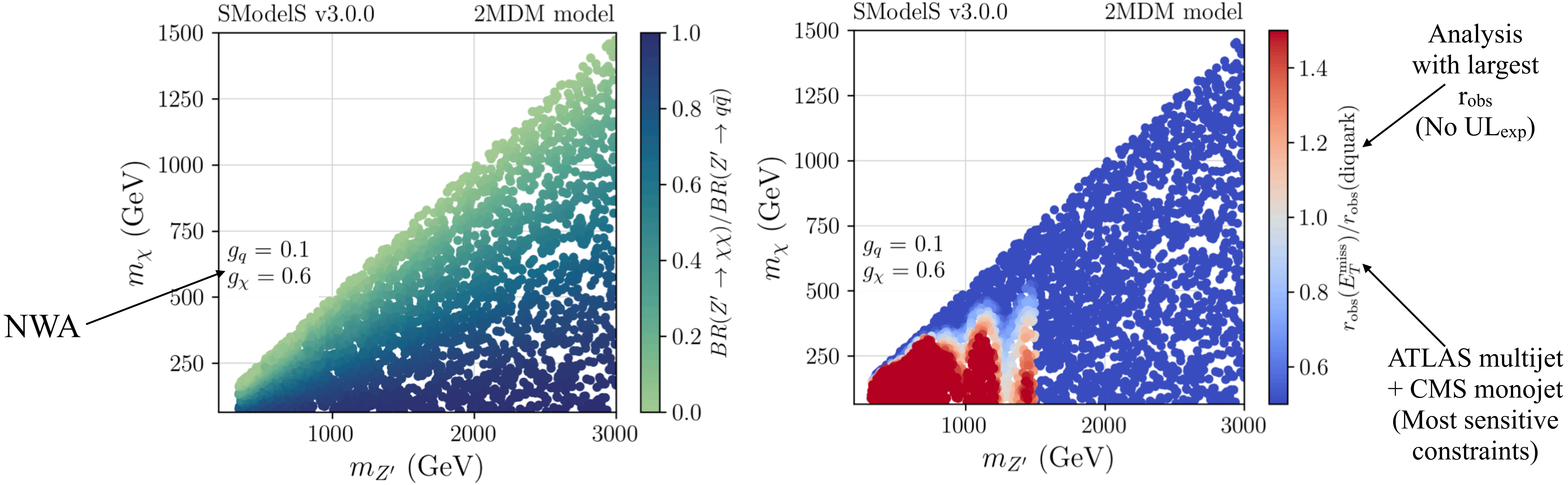

- $m_{Z'} < 1.2$ TeV: E_T^{miss} searches dominates (except for $m_\chi \sim m_{Z'}/2$; invisible decay Z' decay becomes kinematically suppressed)

- $m_{Z'} > 1.5$ TeV: di-quark resonance searches take over; ATLAS-EXOT-2019-03 has high constraining power in this region

Resonance vs jets + MET searches

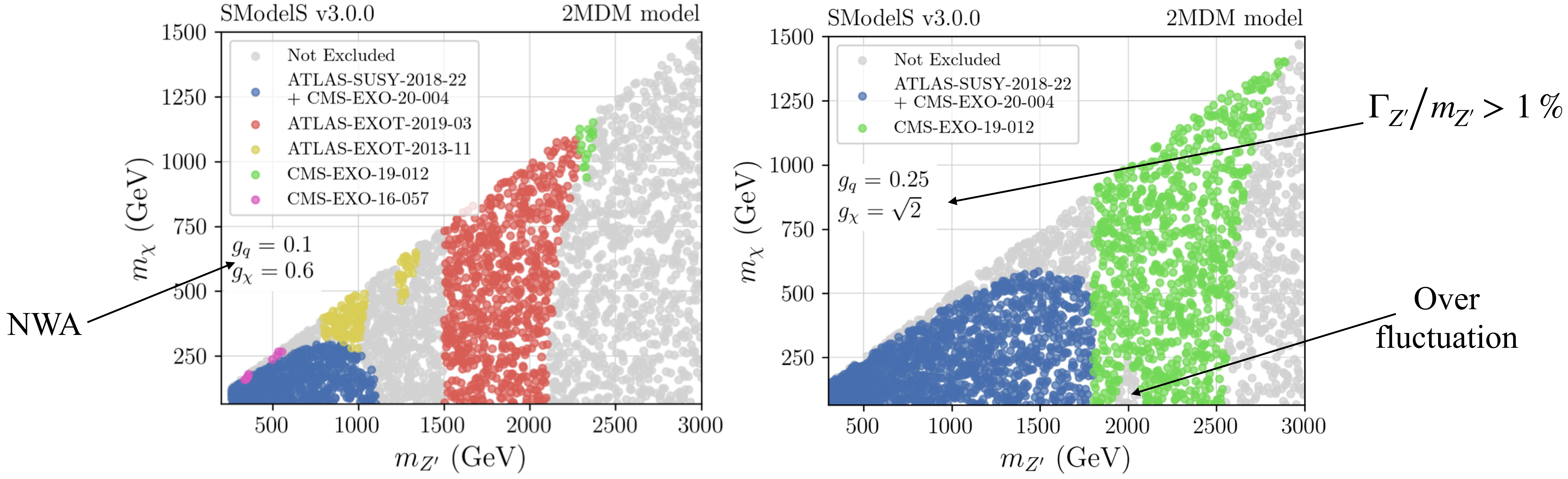

- The colours indicate which is the most constraining analysis (largest r_{obs})
- Larger couplings, larger production cross-section: larger exclusion, larger width: no NWA
- For more accurate and statistically robust conclusions width dependent EM are needed

Conclusions

Conclusions

- **SModelS** is an easy-to-use **public** tool for **fast reinterpretation** of **LHC searches** on the basis of **simplified-model** results
- **Version 3** can now deal with topologies beyond the $\mathbf{Z_2}$ symmetry
- More **EM** type results are needed in order to perform more sophisticated studies
- **Width-dependent** results are very important to reinterpret **resonance searches**
- All results from arXiv:2409.12942 are available on Zenodo
- We thank ATLAS & CMS analyses teams for making their results accessible and reusable!

Backup

slides

Graphical & string representation of SMS in SModelS

- **SModelS** allows for an **interchangeable format** between graph and string representations
- **Graphical representation**:
  - Useful for visualising the **SMS** topologies
  - Provides an intuitive understanding of decay chains but may not be convenient for textual descriptions
- **String format representation**:
  - Uses a sequence of decay patterns: $X(i) \rightarrow A(j), B(k), C(l)$
    - X: **BSM** particle undergoing decay; A, B, C: decay products
    - Indices i, j, k, l denote node indices in the **SMS** graph, avoiding ambiguities

Graphical & string representation of SMS in SModelS

- **Concrete example:**
  - **Graphical SMS** example: PV to gluino(1), su_L(2)
    - gluino(1) to N1(3), q(4), q(5)
    - su_L(2) to q(6), N1(7)
  - **Simplified string representation** in **SModelS** output:
    - (PV→ gluino(1), su_L(2)), (gluino(1) → N1, q, q), (su_L(2) → q, N1)
- **Usage & Notation**:
  - **String format** is utilized for specifying **SMS** topologies constrained by experimental results in the **SModelS v3** database
  - Particle names like "gluino" or "N1" are **generic placeholders** for **BSM** particles with appropriate quantum numbers, not necessarily tied to **SUSY** particles (`databaseParticles.py`)

Graph-based topologies: canonical name

- Describes the structure of the **SMS** topology without specifying its particle contents:
  - Each **undecayed (final node)** receives the label: 10
  - Each **decayed node** receives the label: 1<sorted labels of daughter nodes>0
  - The label associated with the **root node** uniquely describes the graph structure

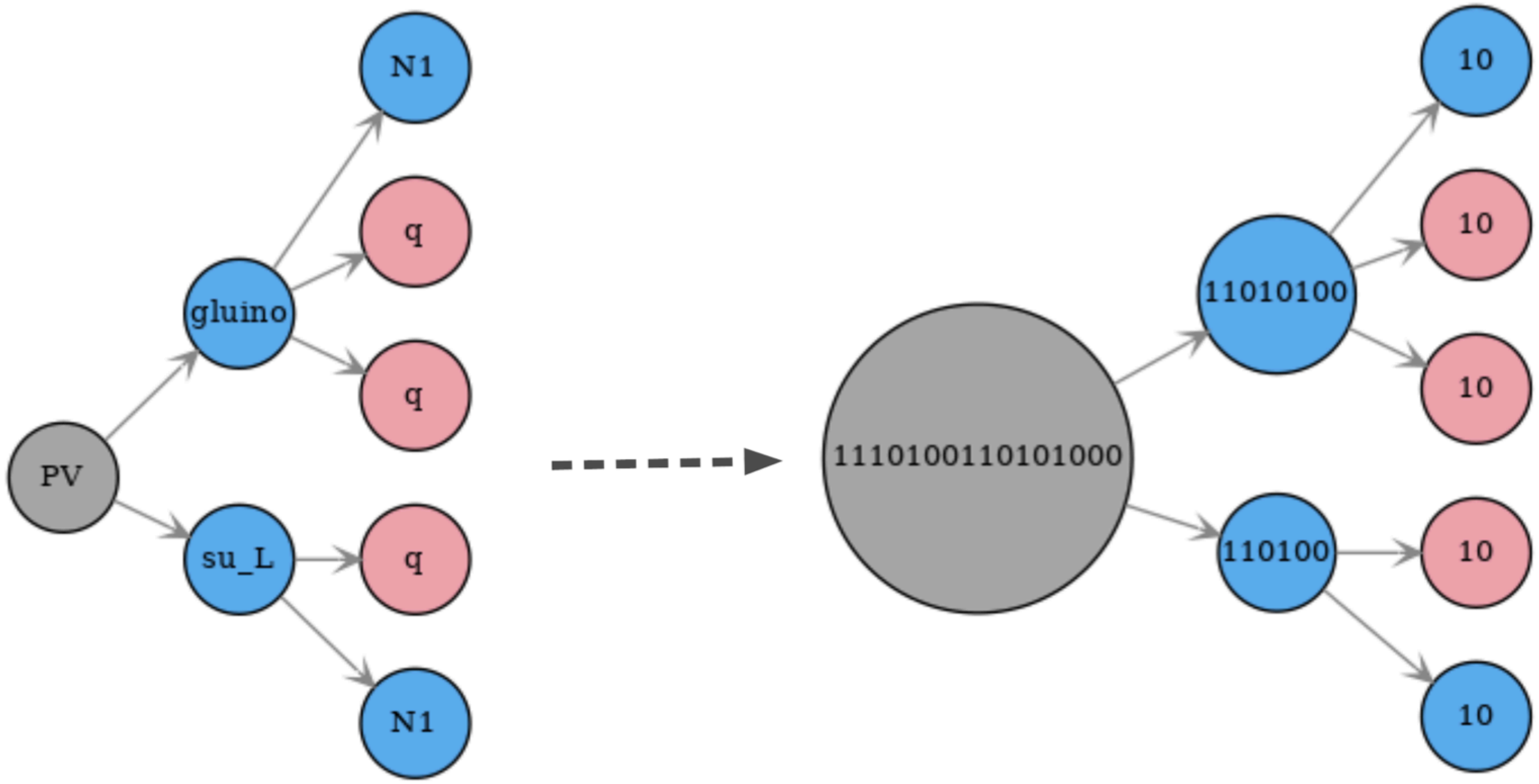

SMS matching: an illustrative example

- **Matching Steps**:
  - Compare **root nodes**:
    - **Canonical names** match (no need to compare particle properties)
  - Compare **daughter nodes** (unordered):
    - Check if (gluino, N1) matches (MET, anyBSM) or (N1, gluino) matches (MET, anyBSM)
    - Result: gluino ↔ anyBSM, N1 ↔ MET
  - **Match daughters** of gluino and anyBSM:
    - Compare (g, N1) with (jet, MET)
    - Result: g ↔ jet, N1 ↔ MET
  - **No more decays**: **stop**, **full match achieved**

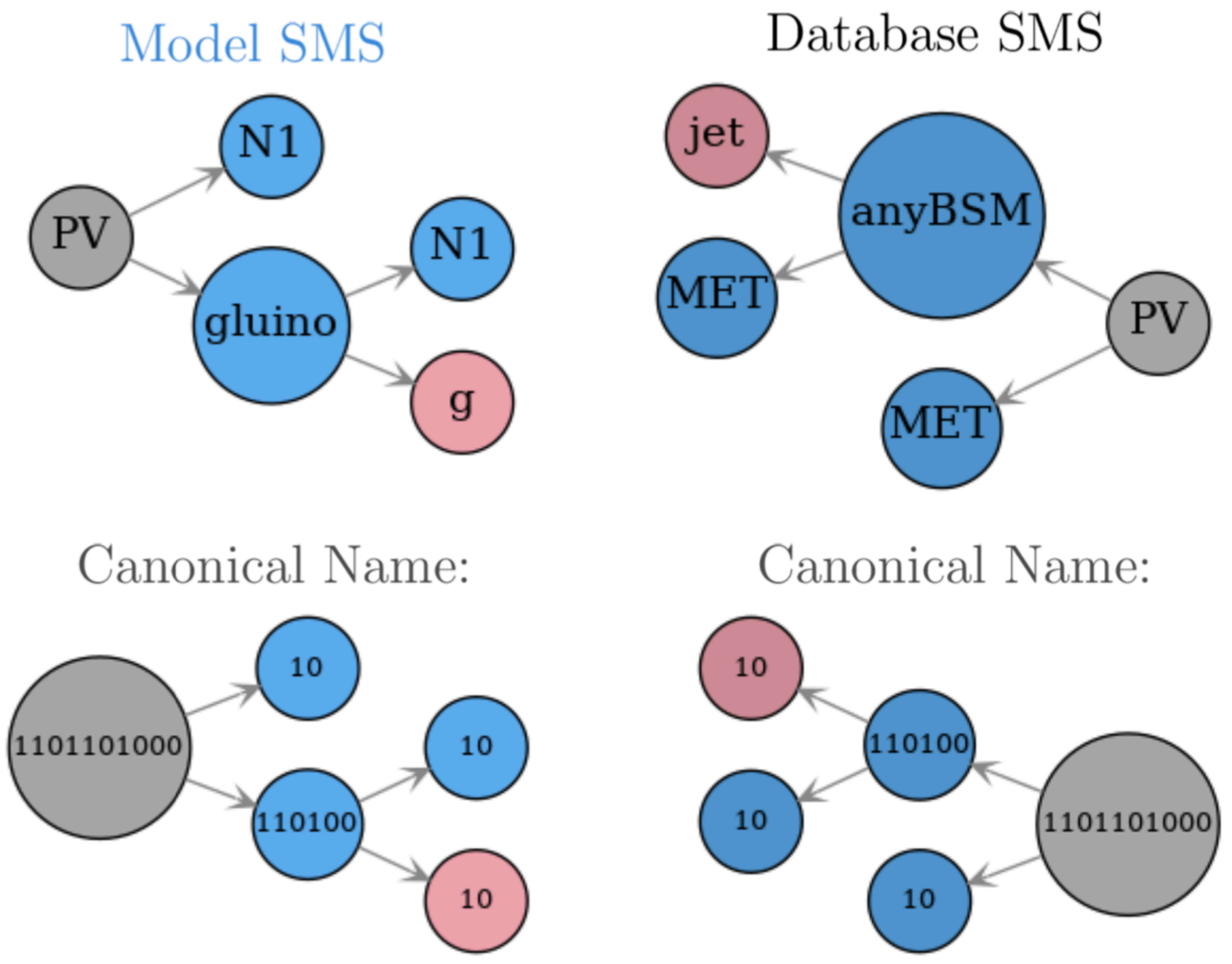

Changes in input model and parameter card

- **Input model definition**:
  - Defines **BSM** particles and their **QN**
  - Can be specified using a **Python** module or an **SLHA** file
  - **Z_2** parity **QN** (No longer required); ignored if included
  - **BSM** particle definition (Python module example):
    - New syntax for defining particles, e.g., for a **left-handed down squark** in **MSSM**:

```
sdl = Particle(isSM=False, label='sd_L', pdg=1000001, eCharge=-1/3, colordim=3, spin=0)
```

Changes in input model and parameter card

- **Input model definition**:
  - **SM** particles:
    - Properties (masses, BRs) are fixed and cannot be modified via input
    - **SM**-like Higgs assumed to have 125 GeV mass and **SM** BRs:
      - Use **PDG** Code 25 only for **SM** Higgs
      - Assign different **PDG** codes for non-**SM**-like scalars
      - **Reason**: Ensures correct matching with experimental results assuming **SM** Higgs decays

Changes in input model and parameter card

- **Parameter card updates**:
  - **New options**:
    - `ignorePromptQNumbers`: Allows ignoring specific **QN** (e.g., spin, electric charge) for promptly decaying particles
    - `outputFormat`: New default string representation; old bracket notation format available with `outputFormat = version2` option

Changes in the output

- **New String Representation**:
  - Replaces old bracket notation with a more compact string format for **SMS** topologies
  - Converts back to bracket notation if `outputFormat = version2` is set (for $\mathbf{Z_2}$ symmetry cases)
- **More compact & informative**:
  - Particle masses information is displayed as a list of tuples, so it is clear which **BSM** particles the masses refer to
- **Graphical output option**:
  - Users can generate visual representations of **SMS** topologies using the **SModelS** Python library

Changes in the output

Version 2:

```
Element ID: 1
Particles in element: [[[higgs]], [[W-]]]
Final states in element: [N1, N1~]
The element masses are
Branch 0: [2.69E+02 [GeV],1.29E+02 [GeV]]
Branch 1: [2.69E+02 [GeV],1.29E+02 [GeV]]

The element PIDs are
PIDs: [1000023,1000022]
PIDs: [1000024,1000022]
The element weights are:
  Sqrts: 1.30E+01 [TeV], Weight:3.92E-01 [pb]
  Sqrts: 8.00E+00 [TeV], Weight:1.74E-01 [pb]
```

Version 3:

```
SMS ID: 1
SMS: (PV > N2(1),C1-(2)), (N2(1) > N1,higgs), (C1-(2) > N1\,,W-)
Masses: [(N2, 2.69E+02 [GeV]), (C1-, 2.69E+02 [GeV]), (N1, 1.29E+02 [GeV]),
         (N1\,, 1.29E+02 [GeV])]
Cross-Sections:
  Sqrts: 1.30E+01 [TeV], Weight:3.92E-01 [pb]
  Sqrts: 8.00E+00 [TeV], Weight:1.74E-01 [pb]
```

Two-Mediator Dark Matter (2MDM) model

- The lagrangian of the **2MDM** model:

$$\mathcal{L} = \mathcal{L}_{\rm SM} + \mathcal{L}_{Z'} + \mathcal{L}_{\phi} + \mathcal{L}_{\chi}$$

- With:

$$\mathcal{L}_{Z'} = g_{Z'} q_q \sum_q \bar{\psi}_q \gamma_\mu \psi_q Z'^\mu - \frac{1}{4} F'^{\mu\nu} F'_{\mu\nu} - \frac{1}{2} \sin\epsilon\, F'^{\mu\nu} B_{\mu\nu}\,,$$

$$\mathcal{L}_{\phi} = \left(\mathcal{D}^\mu \phi\right)^\dagger \left(\mathcal{D}_\mu \phi\right) - \mu_2^2 |\phi|^2 - \lambda_2 |\phi|^4 - \lambda_3 |\phi|^2 |H|^2\,,$$

$$\mathcal{L}_{\chi} = \frac{i}{2} \overline{\chi} \not{\partial} \chi - \frac{1}{2} g_{Z'} q_\chi Z'^\mu \overline{\chi} \gamma^5 \gamma_\mu \chi - \frac{1}{2} y_\chi \overline{\chi} \left(P_L \phi + P_R \phi^*\right) \chi$$

- The mixing angle ϵ between Z' and the hypercharge gauge boson B is set to zero due to stringent experimental constraints

- The last term in $\mathcal{L}_\chi$ ensures a mass for χ and requires $q_\phi = -2q_\chi$

Two-Mediator Dark Matter (2MDM) model

- The scalar S and the **SM** Higgs h correspond to linear combinations of the neutral components of ϕ and H:

$$h = H^0 \cos\alpha - \phi^0 \sin\alpha$$
$$S = \phi^0 \cos\alpha + H^0 \sin\alpha$$

- The **BSM** masses are given by:

$$m_{Z'} = 2 g_{Z'} q_\chi v_2\,, \ m_S^2 = m_h^2 + 2\frac{\lambda_3}{\sin 2\alpha} v v_2\,, \ \text{and } m_\chi = \frac{y_\chi}{\sqrt{2}} v_2$$

- Thus:

$$y_\chi = 2\sqrt{2}\ g_{Z'} q_\chi\ \frac{m_\chi}{m_{Z'}}$$

Two-Mediator Dark Matter (2MDM) model

- Feynman rules for the relevant interactions of Z', S and χ:

Interaction	Vertex term
$Z'_\mu\, q\, \bar{q}$	$i g_q \gamma^\mu$
$Z'_\mu\, \chi\, \chi$	$-i g_\chi \gamma^\mu \gamma^5$
$S\, f\, \bar{f}$	$-i \frac{m_f}{v} \sin\alpha$
$S\, \chi\, \chi$	$-2 i g_\chi \frac{m_\chi}{m_{Z'}} \cos\alpha$
$S\, W^-_\mu\, W^+_\nu$	$2 i g^{\mu\nu} \frac{m_W^2}{v} \sin\alpha$
$S\, Z_\mu\, Z_\nu$	$2 i g^{\mu\nu} \frac{m_Z^2}{v} \sin\alpha$
$S\, h\, h$	$-i \frac{m_S^2}{2 m_{Z'} v} \left(1 + 2\frac{m_h^2}{m_S^2}\right) (m_{Z'} \cos\alpha + 2 g_\chi v \sin\alpha) \sin(2\alpha)$
$S\, Z'_\mu\, Z'_\nu$	$4 i g^{\mu\nu} g_\chi m_{Z'} \cos\alpha$

Two-Mediator Dark Matter (2MDM) model

- The decay widths:

$$\Gamma(Z' \to q\bar{q}) = \frac{g_q^2 m_{Z'}}{4\pi}\sqrt{1-\frac{4m_q^2}{m_{Z'}^2}}\left(1+\frac{2m_q^2}{m_{Z'}^2}\right),$$

$$\Gamma(Z' \to \chi\chi) = \frac{g_\chi^2 m_{Z'}}{24\pi}\left(1-\frac{4m_\chi^2}{m_{Z'}^2}\right)^{3/2}.$$

$$\Gamma(S \to \ell\bar{\ell}) = \frac{m_S}{16\pi}\frac{m_l^2}{v^2}\left(1-\frac{4m_\ell^2}{m_S^2}\right)^{3/2}\sin^2\alpha\,,$$

$$\Gamma(S \to q\bar{q}) = 3\frac{m_S}{16\pi}\frac{m_q^2}{v^2}\left(1-\frac{4m_q^2}{m_S^2}\right)^{3/2}\sin^2\alpha\,,$$

$$\Gamma(S \to \chi\chi) = g_\chi^2\frac{m_S}{4\pi}\frac{m_\chi^2}{m_{Z'}^2}\left(1-\frac{4m_\chi^2}{m_S^2}\right)^{3/2}\cos^2\alpha\,,$$

$$\Gamma(S \to WW) = \frac{m_S^3}{16\pi v^2}\sqrt{1-\frac{4m_W^2}{m_S^2}}\left(1-\frac{4m_W^2}{m_S^2}+\frac{12m_W^4}{m_S^4}\right)\sin^2\alpha\,,$$

$$\Gamma(S \to ZZ) = \frac{m_S^3}{32\pi v^2}\sqrt{1-\frac{4m_Z^2}{m_S^2}}\left(\frac{4m_Z^2}{m_S^2}-\frac{12m_Z^4}{m_S^4}-1\right)\sin^2\alpha\,,$$

$$\Gamma(S \to hh) = \frac{m_S^3}{128\pi v^2 m_{Z'}^2}\left(1+2\frac{m_h^2}{m_S^2}\right)^2\sqrt{1-\frac{4m_h^2}{m_S^2}}$$

$$\times\,(m_{Z'}\cos\alpha + 2g_\chi v\sin\alpha)^2\sin^2(2\alpha)\,,$$

Why we exclude the scalar production

- The spin-0 production cross-section is typically much smaller than the spin-1 cross section, unless $g_q \ll \sin\alpha$ and/or $m_S \ll m_{Z'}$:

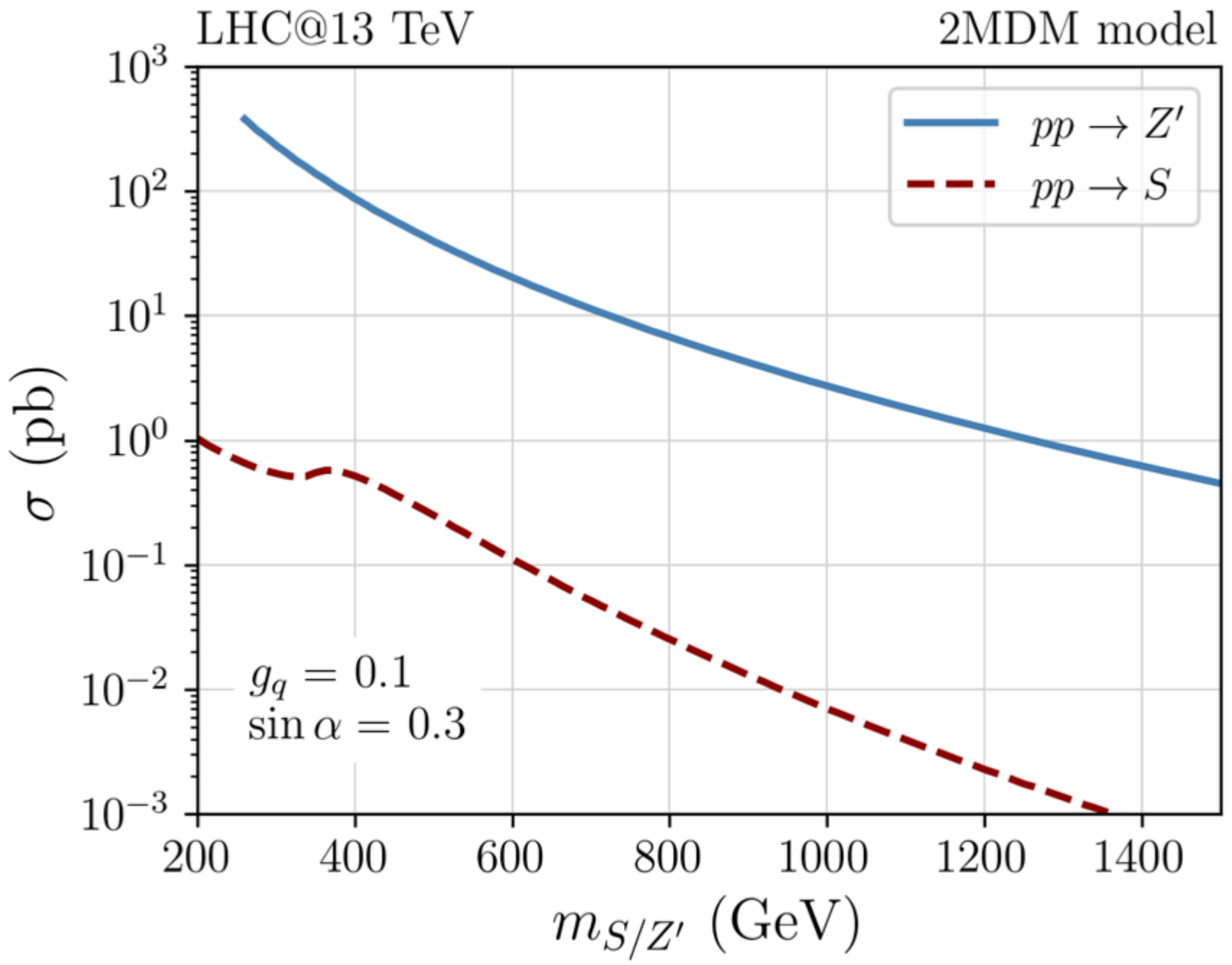

Cross-sections for the resonant production of the spin-1 and spin-0 mediators at the **LHC**. The Z' coupling to quarks is fixed to $g_q = 0.1$, while the S–h mixing angle is $\sin\alpha = 0.3$ Computed at leading order using MadGraph5

Why we exclude the scalar production

- The current limit on α is $\sin\alpha < 0.27$ arXiv:2305.16169
- Even if we saturate this bound the S production cross-section is too small to be probed by resonance or E_T^{miss} searches
- The expected r-value $\left(r_{exp}^{max} = \sigma(pp \to S) / \sigma_{UL}^{exp}\right)$ is much smaller than 1, indicating no potential exclusion by the CMS monojet search

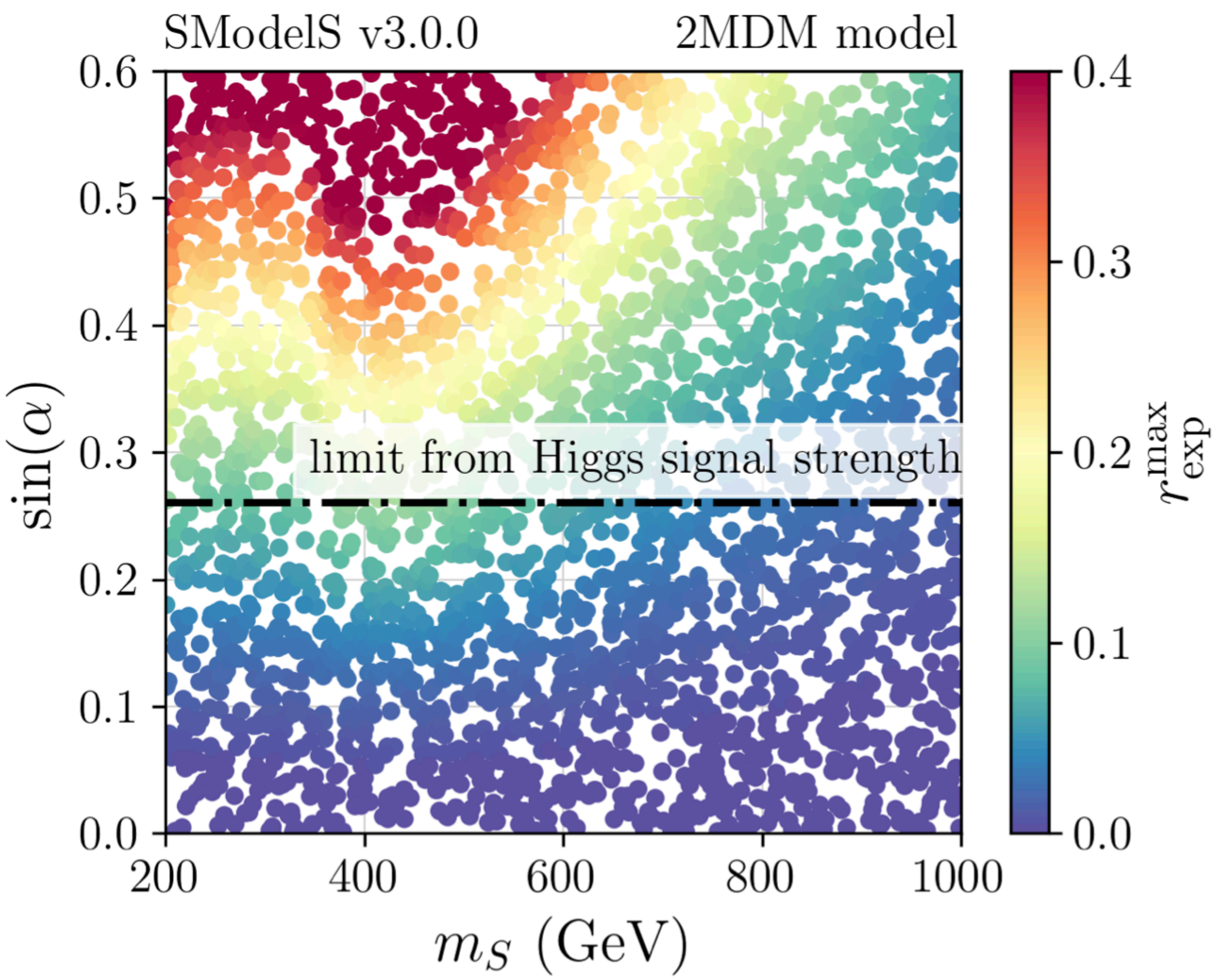

Ratio of S production cross-section to its expected 95% **CL** upper limit from CMS-EXO-20-004. The dashed black line denotes the limit from Higgs signal strength measurements. (r_{exp}^{max}: BR$(S \to \chi\chi) = 100\,\%$).

Parameter scan

- Note on the Z' width:
  - Large for high values of g_q and g_χ; **NWA** not valid
    - Only CMS-EXO-19-012 provides width dependent results; other resonance searches can only be used in the **NWA**
    - E_T^{miss} + jets searches valid up to $\Gamma_{Z'}/m_{Z'} \simeq 5\,\%$
- $\Gamma_{Z'}/m_{Z'}$ always larger than $1\,\%$, can reach up to $5.6\,\%$

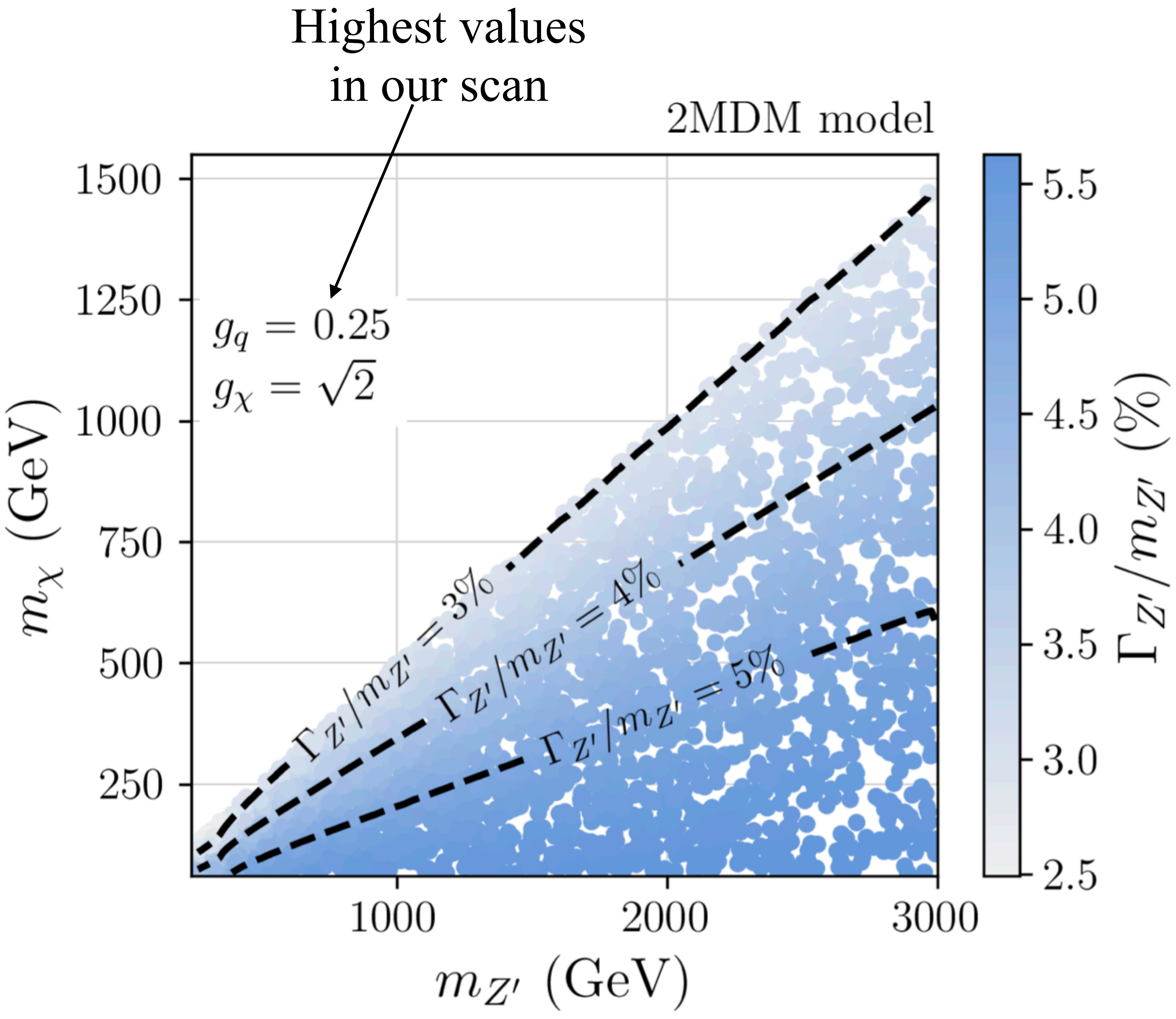

Constraints from jets + MET searches

- In the **NWA** & for $m_\chi \ll m_{Z'}$ the signal in the E_T^{miss} channel is $\propto g_q^2 \dfrac{1}{1 + g_q^2/g_\chi^2}$
  - For fixed g_q the signal increases with g_χ
  - For fixed g_χ the signal increases with g_q
  - Altogether, the signal increases or decreases with both g_q and g_χ

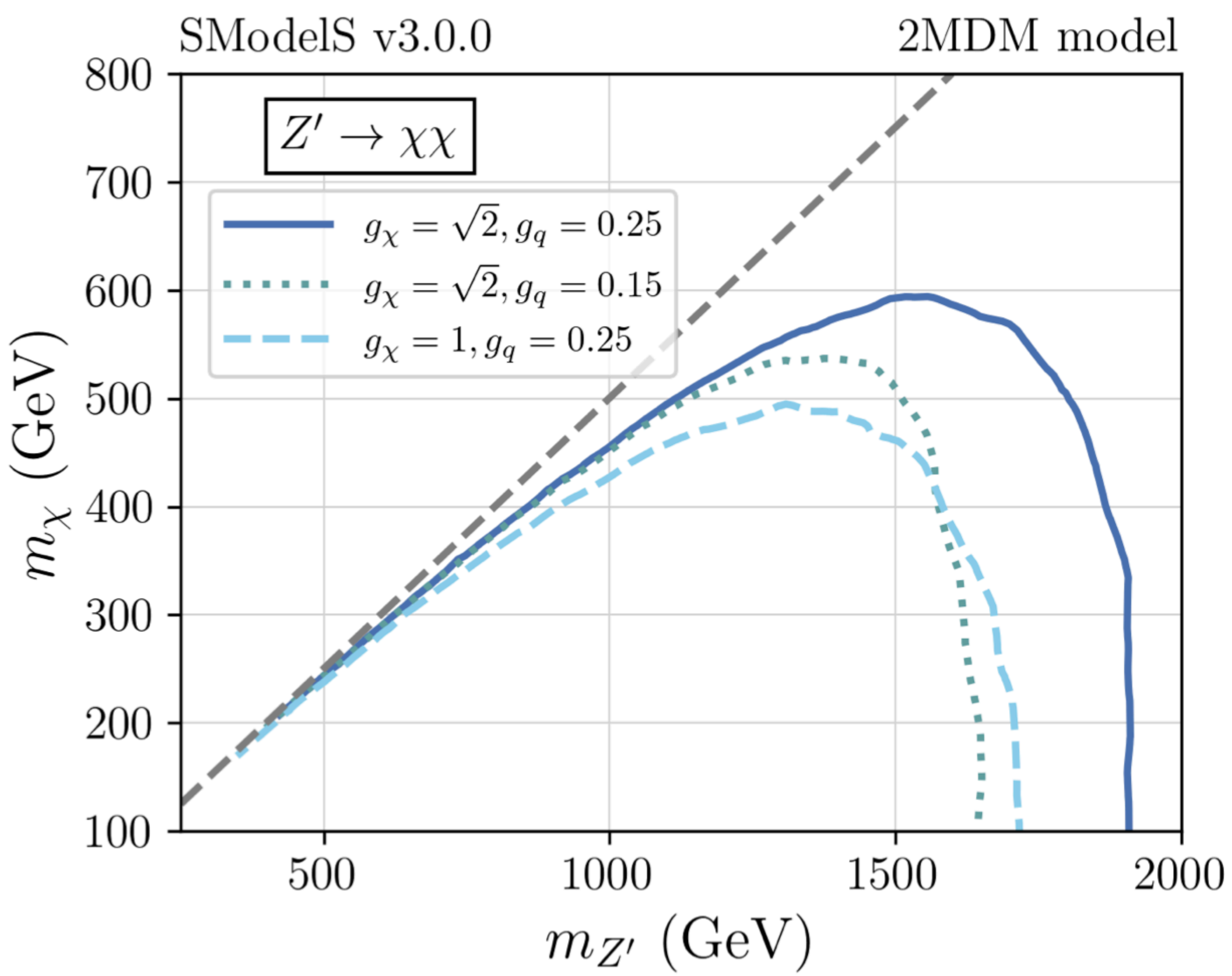

Exclusion lines in the from the combination of the ATLAS multijet and the CMS monojet searches, for three different choices of couplings

Constraints from di-quark resonance searches

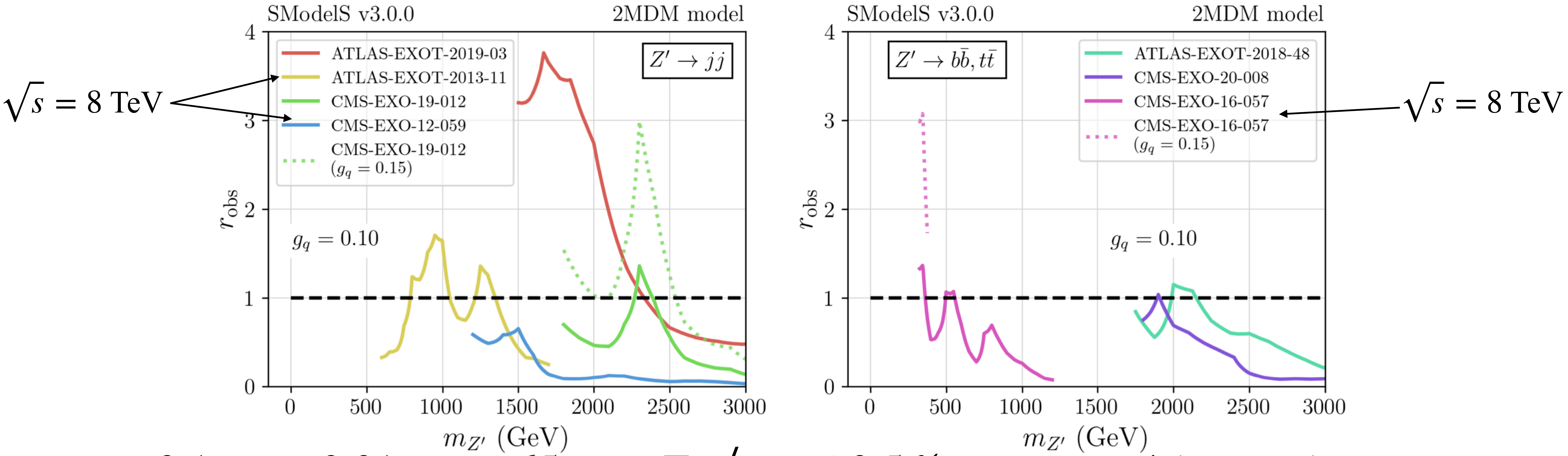

- $g_q = 0.1$, $g_\chi = 0.01$, $m_\chi = 65$ GeV, $\Gamma_{Z'}/m_{Z'} \lesssim 0.5\,\%$: **NWA** & Z' decays almost exclusively to jj, $b\bar{b}$ and $t\bar{t}$ (if kinematically allowed)

- $g_q = 0.15$, $\Gamma_{Z'}/m_{Z'} > 1\,\%$ (no **NWA** for $m_{Z'} > 300$ GeV): more information is needed from experimentalists

Constraints from di-quark resonance searches

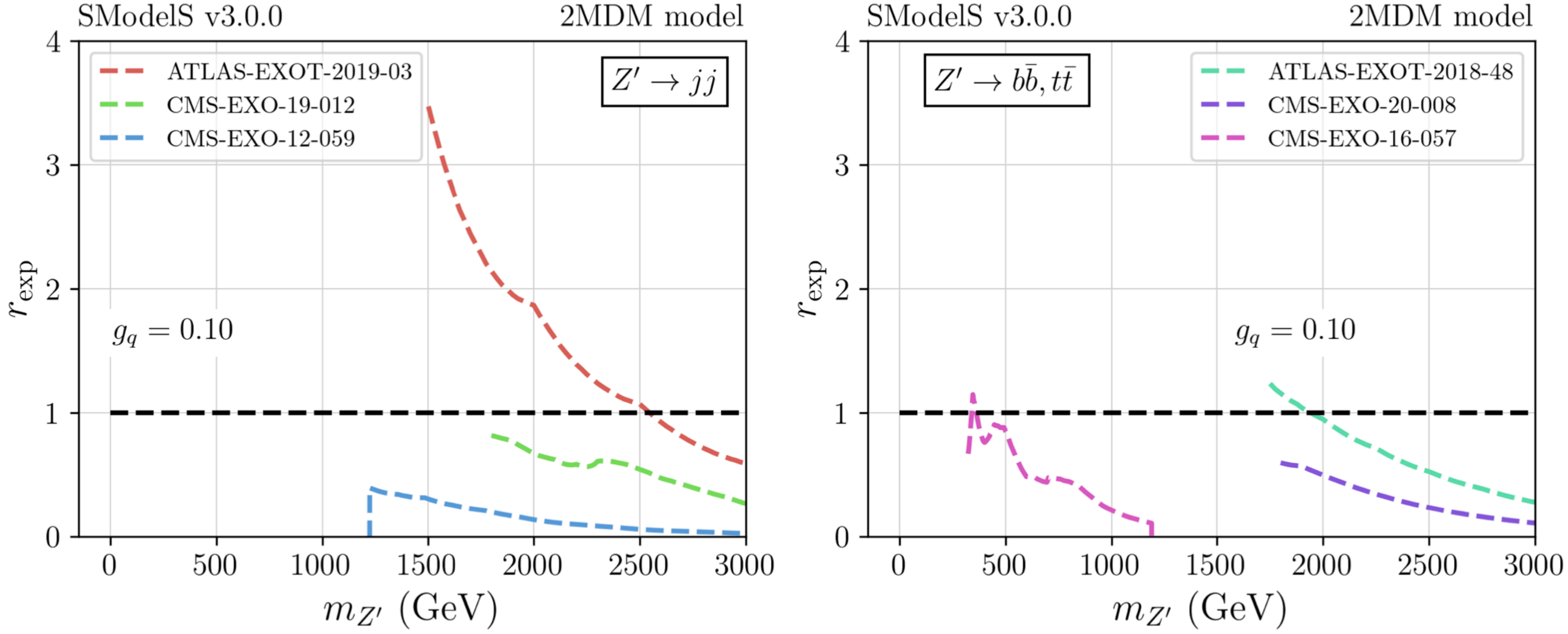

- ATLAS-EXOT-2019-03 is more sensitive than CMS-EXO-19-012
- ATLAS-EXOT-2018-48 is more sensitive than CMS-EXO-20-008
- ATLAS-EXOT-2019-03 is the most sensitive for high-mass range
- Combining ATLAS and CMS dijet searches would average out fluctuations and provide more robust limits